Disks and Jets

John F. Hawley, Christian Fendt, Martin Hardcastle, Elena Nokhrina & Alexander Tchekhovskoy

Space Science Reviews

ISSN 0038-6308

Space Sci Rev
DOI 10.1007/s11214-015-0174-7

Springer

Your article is protected by copyright and all rights are held exclusively by Springer Science +Business Media Dordrecht. This e-offprint is for personal use only and shall not be self-archived in electronic repositories. If you wish to self-archive your article, please use the accepted manuscript version for posting on your own website. You may further deposit the accepted manuscript version in any repository, provided it is only made publicly available 12 months after official publication or later and provided acknowledgement is given to the original source of publication and a link is inserted to the published article on Springer's website. The link must be accompanied by the following text: "The final publication is available at link.springer.com".

Author's personal copy

Space Sci Rev
DOI 10.1007/s11214-015-0174-7

Disks and Jets

Gravity, Rotation and Magnetic Fields

John F. Hawley[1] · Christian Fendt[2] · Martin Hardcastle[3] · Elena Nokhrina[4] · Alexander Tchekhovskoy[5]

Received: 26 November 2014 / Accepted: 11 June 2015
© Springer Science+Business Media Dordrecht 2015

Abstract Magnetic fields are fundamental to the dynamics of both accretion disks and the jets that they often drive. We review the basic physics of these phenomena, the past and current efforts to model them numerically with an emphasis on the jet-disk connection, and the observational constraints on the role of magnetic fields in the jets of active galaxies on all scales.

Keywords Accretion · Accretion disks · Black hole physics · Jets · MHD · Instabilities

1 Introduction

The topic of this workshop was the diverse astrophysical phenomena enabled by the strongest magnetic fields in the Universe. Gamma ray bursts and magnetars provide two

A. Tchekhovskoy is an Einstein Fellow.

✉ J.F. Hawley
jh8h@virginia.edu

C. Fendt
fendt@mpia.de

M. Hardcastle
m.j.hardcastle@herts.ac.uk

E. Nokhrina
nokhrinaelena@gmail.com

A. Tchekhovskoy
atchekho@berkeley.edu

1 Department of Astronomy, University of Virginia, Charlottesville, USA

2 Max Planck Institute for Astronomy, Königstuhl 17, 69117 Heidelberg, Germany

3 School of Physics, Astronomy and Mathematics, U. Hertfordshire, Hatfield, UK

4 Moscow Institute of Physics and Technology, Moscow, Russia

5 Department of Physics and Department of Astronomy, UC Berkeley, Berkeley, CA, USA

Published online: 19 June 2015

Author's personal copy

examples of extreme phenomena where extraordinarily strong fields are manifest. However, the concept of "strong" is relative. A magnetic field may be weak in the sense that the energy density associated with the field is small compared to other energies, e.g., thermal, rotational, gravitational. Such "weak" magnetic fields can, however, enable phenomena that otherwise would not be possible. In this contribution we consider just such an example, namely accretion disks and the jets they produce. Magnetic fields are fundamental to both accretion and outflows, and while in some specific cases the magnetic fields may be strong in the conventional sense of total energetics, for the most part the fields are likely to be relatively weak by those same conventional metrics. Nevertheless, magnetic fields play the central dynamic role.

Gravity is the dominant force in creating the structure in the universe. When gravity is combined with angular momentum, the result is a disk. Since some angular momentum will inevitably be present, disks are arguably the most basic type of object in the universe. Other structures, such as stars, result from disks that have somehow shed most of their angular momentum. Accretion is also a major astrophysical power source. As Lynden-Bell observed (Lynden-Bell 1969), the gravitational energy available in black hole accretion greatly exceeds that available through nuclear reactions, with efficiencies anywhere from 6–40 % mc^2, versus less than 1 % for nuclear fusion.

Direct observational evidence for magnetic fields in accretion disks is very limited (measurements exist, e.g., for FU Orionis, Donati et al. 2005). The strongest case for magnetic fields is theoretical. We know from observations that disks accrete at rates that require considerable internal stress to transport angular momentum. As we shall discuss, this requires magnetic fields.

Indirect evidence for magnetic fields in accreting systems comes from observations of highly collimated outflows, or jets. Jets are one of the most striking signatures resulting from accretion, and are seemingly ubiquitous; they are associated with young stars, micro-quasars or X-ray binaries (MQs, XRBs), and active galactic nuclei (AGN). The current understanding of jet formation is that outflows are launched by *magnetohydrodynamic* (MHD) processes in the close vicinity of the central object (Blandford and Payne 1982; Pudritz and Norman 1983; Pudritz et al. 2007; Shang et al. 2007) It is furthermore clear that accretion and ejection are related to each other. Jets may be a consequence of accretion, but accretion may, in turn, be a consequence of a jet. Accretion occurs when gas loses some of its angular momentum, and one very efficient way to remove angular momentum from a disk is to eject it vertically into a jet or outflow (Wardle and Königl 1993; Ferreira and Pelletier 1993; Li 1995; Ferreira 1997). Not all details of the physical processes involved are completely understood yet.

In stellar sources, a central stellar magnetic field is surrounded by a disk carrying its own magnetic flux. Such a geometrical setup can be found in young stars, cataclysmic variables, high-mass and low-mass X-ray binaries, and other micro-quasar systems. Systems such as AGN or μ-quasars have a black hole at their center, and a black hole cannot have an intrinsic magnetic field. The surrounding accretion disk, however, can support the magnetic flux needed for jet launching. In this case, the interaction of the black hole itself with the ambient field may launch a highly magnetized Poynting flux-driven axial flow (Blandford and Znajek 1977).

Although jets are found in a wide range of systems, from protostars to AGN, from the observational point of view protostellar and relativistic jets are quite different. For protostars we can measure Doppler-shifted forbidden line emission to obtain gas velocities, densities or temperatures, and these provide a good estimate on the mass flux of the outflow. Evidence concerning the magnetic field, however, is mainly indirect: magnetic flares of large-scale

Author's personal copy

protostellar stellar magnetic fields indicate that protostellar jets originating from an area close to the star, originate in a magnetized environment. As noted above, in a few objects there are direct measurements of the strength or orientation of magnetic fields in the disks (e.g. Donati et al. 2005; Stephens et al. 2014). Concerning the jet magnetic field, direct evidence is less clear. So far an estimate is available for only one source, HH80/81, obtained from observed synchrotron emission (Carrasco-González et al. 2010). The situation is completely reversed for relativistic jets. While there is plenty of information concerning the jet magnetic field structure, and some constraints on field strengths, speeds are harder to measure, there is no direct measure of the mass fluxes involved, and the magnetic properties of the accretion flow are not directly observable. We do not even know for certain whether the matter content of these jets is leptonic or hadronic (Sect. 5).

While protostars and AGN are the most common jet sources known, the typical characteristics of jet systems—the existence of an accretion disk and a strong magnetic field—are also present in other astrophysical sources, namely in cataclysmic variables, high mass or low mass X-ray binaries, and pulsars. Resolved Chandra imaging of the Crab (Hester et al. 2002) and the Vela pulsar (Pavlov et al. 2003) do indeed show elongated, highly time-variable but persistent structures emerging along the rotational axis of these systems. Whether these structures are similar to the jets observed in protostars and AGN or are features intrinsic to the pulsar wind nebula is not yet clear. *Persistent* jets are not widely observed in cataclysmic variables (either in the highly transient dwarf novae or the more stable nova-like objects), although there are reports of unresolved, steep-spectrum radio emission, consistent with jet activity, in both types of system (Körding et al. 2008, 2011). It is not clear why jets are not more commonly observed in these systems, although some jet launching models suggesting explanations exist in the literature (Soker and Lasota 2004). One basic reason may be the lack of axisymmetry in cataclysmic variables, as this is thought to be another major condition to launch a jet for a considerable period of time (Fendt and Cemeljic 1998). Alternatively, the observability of jet-related synchrotron emission depends strongly on the local environment of the jet, and it is possible that the conditions for this emission to be observed are simply not typically met in CVs.

In this workshop proceeding we will review the many fundamental roles played by magnetic fields in accretion and outflows, both from a theoretical and an observational point of view. The principal processes involved in jet formation can be summarized as follows (Blandford and Payne 1982; Pudritz and Norman 1983; Pudritz et al. 2007; Shang et al. 2007),

(1) Jets are powered by gravitational energy released through accretion and by rotational energy of the disk and/or the central star (or black hole). Magnetic flux is provided by the star-disk (or black hole-disk) system, possibly by a disk or stellar dynamo, or by the advection of the interstellar field. The star-disk system also drives an electric current.
(2) Accreting plasma is diverted and launched as a plasma wind (from the stellar or disk surface) coupled to the magnetic field and accelerated magneto-centrifugally.
(3) Inertial forces wind up the poloidal field inducing a toroidal component.
(4) The jet plasma is accelerated magnetically (conversion of Poynting flux).
(5) The toroidal field tension collimates the outflow into a high-speed jet beam.
(6) The plasma velocities subsequently exceed the speed of the magnetosonic waves. The super-fast magnetosonic regime is causally decoupled from the surrounding medium.
(7) Where the outflow meets the ISM, a shock develops, thermalizing the jet energy.

The overall process as outlined above is complex and takes place over a wide range of both length- and time-scales. Due to this complexity, the aspects of the jet problem have to

Author's personal copy

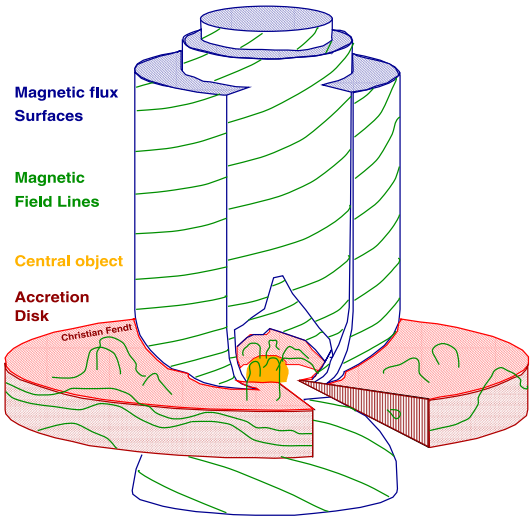

Fig. 1 Model sketch of MHD jet formation, indicating the six generic problems to be solved: launching, acceleration, and collimation; disk structure; magnetic field origin; asymptotic interaction; central spine jet

be tackled independently. One may distinguish six principal topics (Fig. 1), roughly corresponding to the stages in the overall picture described above. These include:

(1) The accretion disk structure and its evolution, including thermal effects and the origin of turbulence.
(2) The origin of the jet magnetic field, possibly through a disk dynamo, a stellar dynamo, or by the advection of ambient magnetic field.
(3) The ejection of disk material into wind, thus the transition from accretion to ejection.
(4) The collimation and acceleration of ejected material into jets.
(5) The propagation of the asymptotic jet, its stability and interaction with ambient medium. A related question is the feedback of jets on star or galaxy formation.
(6) The possible presence and impact of a central spine jet, e.g. a stellar wind or black hole jet, in comparison to a jet originating with the disk. Under what circumstances are disk jets and spine jets present or absent?

In this article we begin by describing the theoretical support for the role of magnetic fields in the accretion disk itself (Sect. 2). We then discuss the modeling of magnetically driven jets (Sect. 3) and their relationship to the disk (Sect. 4). Observational constraints on field properties and their relation to models are discussed in Sect. 5. Our conclusions are presented in Sect. 6.

2 Magnetic Fields and Accretion Disks

We begin with the accretion disk itself, and the fundamental role played by magnetic fields. Throughout the history of disk theory, "shedding the angular momentum" has been easier said than done. The absence of an obvious mechanism to do so was considered a serious objection to Laplace's disk hypothesis for solar system formation, for example. By the time that the basic theory of accretion was laid out by Shakura and Sunyaev (1973) and Lynden-Bell and Pringle (1974) it was accepted that Nature accomplished the transport of angular momentum by some means, though that means was unknown to astronomers. Shakura

Author's personal copy

and Sunyaev introduced the "alpha viscosity" parameterization as a means of sidestepping the uncertainty. In this model the internal stress is proportional to the total pressure, $T_{R\phi} = \alpha P$.

The physical viscosity in the gas within an accretion disk is known to be far too small to account for observed accretion rates. If the disk were turbulent, however, the Reynolds stresses associated with that turbulence could transport angular momentum at the necessary rate. This seemed like a straightforward solution to the problem. Because the viscosity is so small, the Reynolds number (ratio of characteristic velocity times a characteristic length divided by the viscosity) of the gas is correspondingly huge, and in terrestrial contexts high Reynolds number flows are generally turbulent. But gas in Keplerian orbits is stable to perturbations by the Rayleigh criterion, which simply requires that angular momentum increase with radius, $dL/dR > 0$. The positive epicyclic frequency associated with Keplerian orbital flows is strongly stabilizing, and it is not energetically favorable for turbulence to develop and be sustained from the background angular momentum distribution (Balbus et al. 1996; Balbus and Hawley 1998).

The linear stability of Keplerian flows was, of course, recognized early on as a difficulty for the creation of turbulence in disks. However, it was known that in the laboratory simple shear flows display *nonlinear* instability. Balbus et al. (1996) argued that this nonlinear instability represented the boundary between the Rayleigh-stable and Rayleigh-unstable regimes; when the epicyclic frequency goes to zero the linear response vanishes, leaving nonlinear terms as the lowest order effect. Given the importance of the question of the nonlinear stability of hydrodynamic Keplerian flow, several groups have carried out fluid experiments. Ji et al. (2006) examined the stability of a Rayleigh-stable Couette flow and found no evidence of significant turbulence. Paoletti and Lathrop (2011), on the other hand, found a breakdown into turbulence in their experiment. The experiments of Schartman et al. (2012) found no transition to turbulence, and attributed the Paoletti and Lathrop (2011) results to turbulence generated at the end caps of the Couette cylinder, a conclusion further supported by the numerical simulations of Avila (2012). More recent laboratory experiments by Edlund and Ji (2014) are also consistent with stability. While work will no doubt continue on this important issue, at the moment the weight of the theoretical and experimental data lie with the nonlinear hydrodynamic stability of Keplerian flow.

2.1 Basic MRI Physics

It was, of course, recognized early on that magnetic fields could transport angular momentum through Maxwell stresses, $-B_r B_\phi/4\pi$, but unless the magnetic pressure were near the thermal pressure, it was expected that the effective α would be relatively small. As it turns out, magnetic fields render the disk linearly unstable to the *magneto-rotational instability* (Balbus and Hawley 1991, MRI) even when (and, indeed, *only* when) the magnetic field is weak. The MRI can be visualized intuitively in the form of a spring connecting two orbiting masses (Balbus and Hawley 1998), one in a slightly lower orbit than the other. Because angular velocity decreases with R, $\Omega \propto R^{-3/2}$, the inner mass pulls ahead of the outer mass. This causes the spring to stretch; the tension force pulls back on the inner mass, and pulls forward on the outer. The effect of this is to transfer some angular momentum from the inner to the outer mass, but in doing so the inner mass drops to a lower orbit, increasing its angular velocity, increasing the relative separation of the masses and increasing the spring tension force. The process runs away unless the spring is strong enough to force the masses to remain together, which happens only if the tension exceeds the orbital dynamical force. If we replace the spring with a magnetic field, the spring tension is replaced with the magnetic

Author's personal copy

tension associated with the Maxwell stress. In a magnetized disk the linear stability requirement is no longer the Rayleigh criterion, but is instead a requirement that angular *velocity* increase outward, $d\Omega/dR > 0$. A Keplerian disk is unstable.

There are several remarkable properties of the MRI. One is that the question of stability does not depend on the magnetic field strength or orientation. The stability criterion,

$$(\mathbf{k} \cdot \mathbf{v_A})^2 > -\frac{d\Omega^2}{d \ln R}, \tag{1}$$

includes the magnetic field through the Alfv́en speed $\mathbf{v_A}$ but only in combination with a wavenumber vector $\mathbf{k}$. Hence, for any magnetic field, however weak, one can find an unstable wavenumber so long as Ω decreases with R.

The stability criterion for a Keplerian disk is

$$\frac{2\pi}{\lambda_{\rm MRI}} v_A > \sqrt{3}\Omega, \tag{2}$$

which indicates that the unstable wavelengths, $\lambda_{\rm MRI}$, are those that are longer than the distance an Alfvén wave travels in one orbit. The growth rate of the MRI is proportional to $k \cdot v_A$, peaking at a value of $\frac{3}{4}\Omega$ for Keplerian disks for a wavelength (Balbus and Hawley 1998)

$$\lambda_{\rm MRI} = \frac{4}{\sqrt{15}} \frac{2\pi v_A}{\Omega}. \tag{3}$$

As a practical matter, for an increasingly weak field, $\lambda_{\rm MRI}$ should eventually fall to a scale small enough that ideal MHD no longer applies. When the MRI wavelengths are comparable to the resistive scale, for example, the field diffuses through the gas faster than the instability can grow, resulting in stabilization. At the other extreme, namely the strong field limit, the shortest unstable wavelength must fit into the disk. When $\lambda_{\rm MRI}$ is comparable to the scale height of the disk, H, then $v_A \sim c_s$, where c_s is the sound speed. This is a strong field indeed, and this condition is often expressed in terms of the plasma β parameter, which is the ratio of the thermal to magnetic pressure, as $\beta \leq 1$. Strong fields do not necessarily mean a stable, quiet disk, however. First, when $\beta < 1$ the fields are dynamically important and can transport angular momentum directly, possibly through a wind or a jet (see, for example, Lesur et al. 2013). Second, the stability condition on a toroidal field requires the Alfvén speed to be comparable to the *orbital* speed, rather than the sound speed; confining fields of this strength within a disk would seem to be problematic.

To conclude, disks for which the gas has sufficient conductivity as to be magnetized will be linearly unstable to the MRI. The action of the MRI is to transfer angular momentum outward through the disk, precisely what is needed for accretion.

2.2 MRI-Driven Turbulence

The linear analysis establishes that Keplerian orbits are unstable in the presence of a weak magnetic field. For any further understanding of the properties of an unstable disk we must turn to numerical simulations. Accretion simulations can be global or local. Global simulations model the whole disk, or at least a region of significant radial extent. Local simulations, on the other hand, attempt to focus on the properties of the gas within a small region of the disk. For accretion disks, local simulations use an approximation known as the *shearing box* (Hawley et al. 1995). The shearing box domain is assumed to be centered at some radial location R that has an orbital frequency $\Omega(R)$. The size of the box is taken to be much less than R so that one can assume a local Cartesian geometry. The tidal gravitational and

Author's personal copy

Coriolis forces are retained. Radial boundary conditions are established by assuming that the box is surrounded by identical boxes sliding past at the appropriate shear rate. Through use of the shearing box approximation one can study the details of MRI-driven turbulence on scales that are much smaller than the scale height of the disk or the radial distance from the central star.

Extensive shearing box simulations have led to the following general conclusions:

- The MRI leads to MHD turbulence characterized by an anisotropic stress tensor: the $R\phi$ magnetic stress component, $T_{R\phi}$, is large, which leads to significant radial transport of net angular momentum (Hawley et al. 1995).
- A net Reynolds stress is also present in the turbulence, and it too transports angular momentum, but the Maxwell stress is consistently larger than the Reynolds stress by a factor of 3–4. If the magnetic fields are removed, the turbulence quickly dies out (Hawley et al. 1995).
- Time and space variations in the turbulence can be large. The turbulence is chaotic (Winters et al. 2003). Characterizing the stress in terms of an α parameter makes sense only in a space- and time-averaged sense.
- The stress is proportional to the magnetic pressure, $T_{R\phi} = \alpha_{\rm mag} P_{\rm mag}$, with an $\alpha_{\rm mag} = 0.4$–0.5. This implies that the traditional Shakura-Sunyaev value is $\alpha \sim 1/\beta$, where β is determined by $P_{\rm mag}$, the total magnetic pressure in the turbulent flow.
- The magnetic energy typically saturates at a value $\beta \sim 10$–100. This is somewhat dependent on the character of the background magnetic field. Simulations with net vertical field tend to saturate at stronger field values.
- The local model is valid in so far as the energy released by the stresses is thermalized promptly, on an eddy turnover time-scale of order Ω^{-1} (Simon et al. 2009). The rapid thermalization of the energy is required for α-disk theory to be applicable (Balbus and Papaloizou 1990).
- The MRI acts like an MHD dynamo in that it sustains positive magnetic field energies in the face of considerable dissipation (Hawley et al. 1996). Further, stratified shearing box simulations exhibit a behavior that can be modeled as an α–Ω dynamo (Brandenburg et al. 1995; Gressel 2010; Guan and Gammie 2011). This is, however, a small-scale dynamo; shearing box simulations have not provided any evidence for the existence of a dynamo capable of producing a large scale field.
- In simulations that include resistivity and viscosity, the amplitude of the MRI-driven turbulent fluctuations and the resulting angular momentum transport are a function of magnetic Prandtl number. Turbulence is not sustained for $P_{\rm M} < 1$ (Lesur and Longaretti 2007; Simon and Hawley 2009), i.e., when the resistivity is greater than the viscosity.

The local simulations tell us a considerable amount about the MRI and the resulting turbulence, but they cannot address questions of a global nature, such as the net accretion rate into the central star, losses due to winds and outflows, and the mechanisms by which jets might be generated. We know, however, that disks will be magnetized, and this implies the possibility of jet generation from the disk. In the next section we discuss the modeling of such jets.

3 Magnetic Jets from Disks—Theory and Simulations

For jet theory and simulation researchers typically consider only a subset of the issues listed in Sect. 1 and employ a variety of simplifications. An early example of a jet simulation

Author's personal copy

that focused on the propagation of the jet and interaction with the surrounding medium is given by Norman et al. (1982) who carried out some of the first high-resolution simulations of hydrodynamic axisymmetric cylindrical jet flows. Some of the earliest simulations of questions related to jet launching, collimation in relation to disk properties were given by Uchida and Shibata (1984) (see also Shibata and Uchida 1985; Uchida and Shibata 1985).

Since those early efforts, considerable work has been done on MHD jet modeling. One may distinguish i) between steady-state models and time-dependent numerical simulations, and also ii) between simulations considering the jet formation only from a fixed-in-time disk surface and simulations considering also the launching process, thus taking into account disk and jet evolution together.

Clearly, many jet properties depend on the mass loading of the jet, which can only be inferred from a treatment of the accretion-ejection process. While numerical simulations of the accretion-ejection structure potentially provide the time-evolution of the launching process, a number of constraints that were found, had been discovered already by previous steady state models (see below).

3.1 Magneto-centrifugal Disk Winds

Steady-state modeling of magneto-centrifugally launched disk winds have mostly followed the self-similar Blandford and Payne (1982) approach (e.g. Contopoulos and Lovelace 1994a; Contopoulos 1994b). Some fully two-dimensional models have been proposed (Pelletier and Pudritz 1992; Li 1993), including some that take into account the central stellar dipole (Fendt et al. 1995). Further, some numerical solutions have been proposed by e.g., Wardle and Königl (1993); Königl et al. (2010); Salmeron et al. (2011) in weakly ionized accretion disks that are threaded by a large-scale magnetic field as a wind-driving accretion disk. They have studied the effects of different regimes for ambipolar diffusion or Hall and Ohm diffusivity dominance in these disk. Self-similar steady-state models have also been applied to the jet launching domain (Wardle and Königl 1993; Ferreira and Pelletier 1993; Li 1995; Ferreira 1997; Casse and Ferreira 2000) connecting the collimating outflow with the accretion disk structure. In particular, the fact that large scale magnetic fields need to be close to equipartition in order to launch jets via the Blandford-Payne mechanism is now well accepted, but was first established with self-similar studies (Ferreira and Pelletier 1993; Li 1995; Ferreira 1997). A similar comment can be made also concerning the turbulent magnetic diffusivity required in accretion disks.

In addition to the steady-state approach, the magneto-centrifugal jet formation mechanism has been the subject of a number of time-dependent numerical studies. In particular, Ustyugova et al. (1995) and Ouyed and Pudritz (1997) demonstrated the feasibility of the MHD self-collimation property of jets. Among these works, some studies have investigated artificial collimation (Ustyugova et al. 1999), a more consistent disk boundary condition (Krasnopolsky et al. 1999; Anderson et al. 2005), the effect of magnetic diffusivity on collimation (Fendt and Cemeljic 2002), the impact of the disk magnetization profile on collimation (Fendt 2006; Pudritz et al. 2006), or the impact of reconnection flares on the mass flux in jets from a two-component magnetic field consisting of a stellar dipole superposed on a disk magnetic field (Fendt 2009).

In the context of core-collapse gamma-ray bursts, Tchekhovskoy et al. (2008) studied the acceleration of magnetically-dominated jets confined by an external medium and demonstrated that jets gradually accelerate under the action of magnetic forces to Lorentz factors $\Gamma \gtrsim 1000$ as they travel from the compact object to the stellar surface. However, Komissarov et al. (2009) pointed out an important problem: such confined, magnetized jets were

Author's personal copy

too tightly collimated for their Lorentz factors to be consistent with observations. Does this mean that gamma-ray burst jets are not magnetically powered? It turns out that magnetized jets are still viable: as they exit the star and become deconfined, they experience an additional, substantial burst of acceleration that brings their properties into agreement with observations (Tchekhovskoy et al. 2010a).

In the context of stellar jets, Ramsey and Clarke (2011) studied the large-scale jet formation process spanning the whole range from the disk surface out to scales of more than 1000 AU. Further extensions of this model approach have included the implementation of radiation pressure by line forces as applied to jets in AGN (Proga et al. 2000; Proga and Kallman 2004) or massive young stars (Vaidya et al. 2011), which may well affect acceleration and collimation of the jet material. Simulations of relativistic MHD jet formation were presented by Porth and Fendt (2010) finding collimated jets just as for the non-relativistic case (above). Applying relativistic polarized synchrotron radiative transport to these MHD simulation data through postprocessing yields mock observations of small-scale AGN jets (Porth et al. 2011).

The stability of the jet formation site has been studied using 3D simulations for the non-relativistic (Ouyed et al. 2003) and the relativistic case (Porth 2013). Self-stabilization of the jet formation mechanism seems to be enforced by the magnetic "backbone" of the jet, the very inner highly magnetized axial jet region. These studies complement simulations investigating the stability of jet propagation on the asymptotic scales. Here, usually a collimated jet is injected into an ambient gas distribution, either for the non-relativistic (Stone and Norman 1992; Todo et al. 1993; Stone and Norman 1994; Stone and Hardee 2000) or the relativistic (Mignone et al. 2010; Keppens et al. 2008) case.

In the aforementioned studies, the jet-launching accretion disk is taken into account as a boundary condition, *prescribing* a certain mass flux or magnetic flux profile in the outflow. This may be a reasonable setup in order to investigate jet formation, i.e. the acceleration and collimation process of a jet. However, such simulations cannot tell the efficiency of mass loading or angular momentum loss from disk to jet, or cannot determine which kind of disks launch jets and under which circumstances.

It is therefore essential to extend the jet formation setup and include the launching process in the simulations—that is, to simulate the accretion-ejection transition. Clearly, this approach is computationally much more expensive. The typical time scales for the jet and disk region differ substantially; disk physics operates on the Keplerian time scale (which increases as $R^{3/2}$), and on the even-longer viscous and the diffusive time scales. The jet follows a much faster dynamical time scale. As this approach is also limited by spatial and time resolution, jet launching simulations to date have employed a rather simple disk model—namely, an α-prescription for the disk turbulent magnetic diffusivity and viscosity, and without considering radiative effects.

Numerical simulations of the launching of MHD jets from accretion disks have been presented by Kudoh et al. (1998); Kato et al. (2002) and Casse and Keppens (2002); Casse and Keppens (2004). These simulations treat the ejection of a collimated outflow out of an evolving disk through which a magnetic field is threaded. To prevent the field from accreting itself, the disk is resistive, allowing the field to slip through. Zanni et al. (2007) further developed this approach with emphasis on how resistive effects modify the dynamical evolution. An additional central stellar wind was considered by Meliani et al. (2006). Further studies have concerned the effects of the absolute field strength or the field geometry, in particular investigating field strengths around and below equipartition (Kuwabara et al. 2005; Tzeferacos et al. 2009; Murphy et al. 2010). These latter simulations follow several hundreds of (inner) disk orbital periods, providing sufficient time evolution to also reach a (quasi) steady state for the fast jet flow.

Author's personal copy

Parameter studies have been able to disentangle the effects of magnetic field strength (magnetization) and magnetic diffusivity (strength, scale height) on mass loading and jet speed (Sheikhnezami et al. 2012). Tzeferacos et al. (2013) considered how entropy affects the launching process, in particular how disk heating and cooling influence the launching process. They find that heating at the disk surface enhances the mass load, as predicted in the steady state modeling by Casse and Ferreira (2000).

Most jets and outflows are observed as *bipolar* streams. Very often, observations show asymmetrical jets and counterjets. For protostellar jets one exception is HH 212, which shows an almost perfectly symmetric bipolar structure (Zinnecker et al. 1998). For relativistic jets Doppler beaming may play a role for the observed jet asymmetries, and, in fact, many well-behaved jets can be modeled on the assumption that Doppler beaming dominates the apparent asymmetry (Laing and Bridle 2014). However, environmental asymmetries must be also considered. It is therefore interesting to investigate the evolution of both hemispheres of a *global* jet-disk system in order to see whether and how a global asymmetry in the large-scale outflow can be governed by the disk evolution. Fendt and Sheikhnezami (2013) have been able to trigger jet asymmetries by disturbing the hemispheric symmetry of the jet-launching accretion disk and find mass flux or jet velocity differences between jet and counter jet of up to 20 %.

von Rekowski et al. (2003) and von Rekowski and Brandenburg (2004) investigated the origin of the magnetic field driving the jet by including a mean-field disk dynamo in the star or in the disk. Asymmetric ejections of stellar wind components were found from offset multi-pole stellar magnetospheres (Lovelace et al. 2010). The most recent work considers the time ($> 5 \times 10^5$ dynamical time steps) evolution on a large spherical grid (> 2000 inner disk radii), including the action of a mean-field disk dynamo that builds up the jet magnetic field. A variable dynamo action may cause the time-dependent ejection of jet material (Stepanovs and Fendt 2014; Stepanovs et al. 2014).

The main jet launching processes seem to be well understood, in the sense that a large number of independent simulation studies give consistent results. Several issues are not yet resolved, however. These include: (i) the origin of jet knots, and (ii) the coupling of the small scale disk physics to the global jet outflow. In the end there is a good chance that the answers to both questions are interrelated. A full numerical simulation that addresses these questions would require substantial effort, including full 3D, high resolution, and more complete physics, in particular the treatment of thermal effects. First steps in this direction have already been taken.

Concerning the origin of jet knots, it is still unclear whether knots are signatures of internal shocks of jet material launched episodically with different speed, external shocks of jet material with the ambient medium, or re-collimation shocks. One observation supporting the intrinsic origin of jet knots is that of the jet of HH 212, which shows an almost perfectly symmetric bipolar structure with an identical knot separation for jet and counter jet (Zinnecker et al. 1998). Such a structure can only be generated by a mechanism intrinsic to the jet source.

The knot separation in protostellar jets typically corresponds to time scales of $\tau_{\rm kin} \simeq$ 10–100 yrs. By contrast, a typical time scale for the jet launching area would be about 10–20 days, that is the Keplerian period close to an inner disk radius of 0.1 AU. This time scale increases up to one year if the jet launching radius is larger, say up to 3–5 AU (Frank et al. 2014). However, outflows launched from such large radii would probably not achieve the high velocities of 300–500 km s^{-1} observed for jets. Thus, the mechanism responsible for the jet knots must be intrinsic to the disk, and triggered by a physical processes on a rather long time scale. Candidates are disk thermal (FU Orionis) or accretion instabilities, a mid-term variation of the jet-launching magnetic field, or MRI-active/dead disks.

Author's personal copy

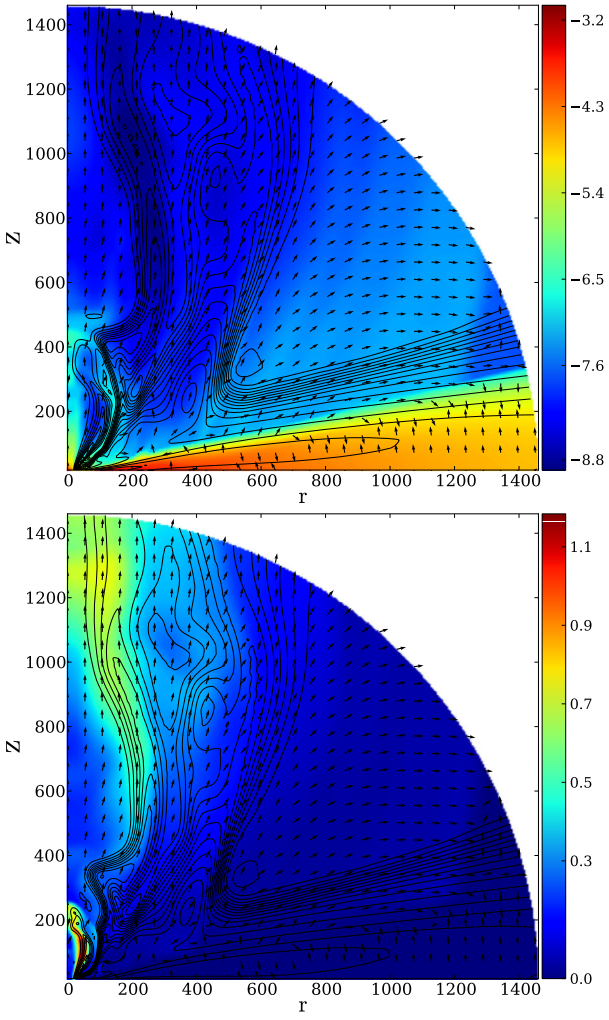

Fig. 2 Time evolution of the inflow-outflow structure for a dynamo-generated disk magnetic field. Shown is the density (*top*, *colors*, in logarithmic scale), and poloidal velocity (*bottom*, *colors*, linear scale), the poloidal magnetic flux (*thin black lines*), and the poloidal velocity vectors. The dynamical time step is about 10^5, while the dynamo time scale (switch on/off) is 10^3. Two ejections of material launched at $\Delta t = 2000$ are more easily seen in the velocity figure (*below*), than in the *top* figure, which shows a slightly later time when the preceding knot has left the grid already. Length units is the inner disk radius of ~ 0.1 AU. Figure taken from Stepanovs and Fendt (2014)

The simulations of Stepanovs et al. (2014) provide an example of episodic knot ejections. They apply an α–Ω mean-field disk dynamo to generate the jet launching magnetic field. In contrary, all previous simulations of this kind start with a strong initial magnetic field distribution. The episodic ejections are triggered by switching on and off the dynamo term every 2000 dynamical time steps (Fig. 2).

The idea of a connection between the small scale disk physics and the global disk outflow is motivated by the fact that jet launching relies on both the existence of a large scale magnetic field and the existence of a (turbulent) magnetic diffusivity, which allows for accretion through the field lines, for angular momentum transfer, and, essentially, also for the mass loading onto the jet magnetic field. The disk turbulence is a result of the magnetorotational instability (MRI, see above) and thus of the small scale physics.

First results combining a mixed numerical-analytical treatment indicate that large scale MRI modes may produce magnetically driven outflows, however, these flows seem to be 3D-unstable (Lesur et al. 2013), and thus may be a transient effect. On the other hand, local

Author's personal copy

numerical simulations suggest that magnetocentrifugal winds can be launched when the MRI is suppressed, in spite of the low magnetization $\sim 10^{-5}$ (Bai and Stone 2013a, 2013b). In this case, outflows are launched from the disk surface region where the plasma β is about unity. This is also what Murphy et al. (2010) have observed in global launching simulations. Lesur et al. (2013) have found that the MRI near equipartition does not lead to turbulence, but can be responsible for jet launching.

The overall goal is still to answer the question: what kind of disks launch jets and what kind of disks do not? It is clear from statistical arguments for both protostars and extragalactic sources that jets are a relatively short-lived phenomenon. The typical jet propagation time scale for protostellar jets is about $\tau_{\rm dyn} \equiv L_{\rm jet}/V_{\rm jet} \simeq 10^4$ yrs, while protostellar disks live some 10^6 yrs. A similar argument can be raised for AGN jets based on the fact that there are far more radio-quiet AGN (quasars) than radio-loud AGN (jet sources), although at least some types of radio-loud AGN appear to be almost continuously in an 'on' state. So far, modeling has not provided an answer to this question.

4 Black Hole Accretion, Fields and Jets

4.1 Simulating the Black Hole Jet

As we have seen, a plethora of models and simulations have demonstrated the ability of magnetic fields to launch, accelerate and collimate jet outflows. But simulations designed to study jets have, as discussed in the previous section, typically used one or another specific set of initial or boundary conditions that pre-suppose a disk structure, a mass-energy flux, a magnetic field configuration, or some combination of these. An alternative approach is to focus not on the jet, but on the accretion disk itself and see when and under what circumstances a jet might *develop* from the flow.

Most global simulations begin with an orbiting axisymmetric hydrostatic equilibrium (torus) a few tens of gravitational radii from the black hole. The initial magnetic field is entirely contained within the matter, so that there is no net magnetic flux and no magnetic field on either the outer boundary or the event horizon. A favorite configuration consists of large concentric dipolar loops (Hawley 2000; McKinney and Gammie 2004; De Villiers et al. 2005; Hawley and Krolik 2006; McKinney 2006). The development of the MRI subsequently leads to the establishment of outflows from the disk. The wind generation seems to be largely an outcome of thermodynamics. In simulations that do not include cooling, the combination of the heat released from accretion and the buildup of magnetic pressure lead to pressure-driven outflows. In the absence of a large scale vertical field through the disk, however, this wind is neither collimated nor unbound.

Global simulations have nevertheless produced jets that are consistent with the Blandford-Znajek mechanism, through the creation of a substantial axial field that threads the black hole. For example, in a model that begins with a torus containing dipolar field loops, differential rotation rapidly generates toroidal field. This field increases the total pressure within the torus, driving the its inner edge inward. As the field is stretched radially, the Maxwell stress transports angular momentum outward, further enhancing the inflow. Subsequent evolution carries the inner edge of the disk, and the magnetic field within, down to the black hole. The field expands rapidly into the nearly empty *funnel* region along the black hole axis. Gas drains off the field lines and into the hole leaving behind a low β axial field. Frame dragging by the rotating hole powers an outgoing Poynting flux. The power of the Poynting flux jet is determined by the spin of the black hole and the strength of the magnetic

Author's personal copy

field (Blandford and Znajek 1977), as we discuss below. The simulated jet's power matches well with the predictions of the Blandford-Znajek model (McKinney and Gammie 2004; McKinney 2005; Tchekhovskoy et al. 2011).

The matter content within the Blandford-Znajek jet is very small; the angular momentum in the disk material is too great to enter the axial funnel. In the simulations the jet density is typically set by the value assigned to the numerical vacuum. How these jets become mass-loaded in Nature is still something of an open issue. Since the boost factor of the jet is determined by the mass loading, Γ is typically large, e.g., $\Gamma \sim 10$ (McKinney 2005). No particular weight can be given to any value of Γ found in simulations, although it is safe to say that the feasibility of values as large as those observed (Sect. 5) has been demonstrated.

Although there is no appreciable matter within the funnel, some of the field lines that lie just outside the funnel pass through the accretion flow, and those field lines can accelerate matter outward in a collimating flow. This "funnel wall jet" was observed in early pseudo-Newtonian simulations (Hawley and Balbus 2002), and is a regular feature of fully relativistic jet simulations, e.g., Hawley and Krolik (2006).

Because the field lines in the jet rotate, the jet carries angular momentum as well as energy away from the black hole. The angular momentum flux can be large, comparable to that brought down by accretion (Gammie et al. 2004; Hawley and Krolik 2006; Beckwith et al. 2008). One potentially important consequence of this was noted by Gammie et al. (2004) who pointed out that electromagnetic angular momentum flux in the jet rises so steeply with black hole spin that it may limit a/M to $\simeq 0.93$ (see also McKinney and Gammie 2004; Hawley and Krolik 2006; Beckwith et al. 2008) or even down to $\lesssim 0.1$, as we discuss below (Tchekhovskoy et al. 2012; Tchekhovskoy 2015). The possibility that magnetic fields could play such an important role in black hole physics is certainly in keeping with the spirit of this workshop!

For a magnetic field strength B at the event horizon, jet power is (roughly) given by the magnetic energy density, B^2, times jet cross-section at its base, r_g^2 (where $r_g = GM/c^2$ is the black hole gravitational radius and M its mass), times the speed $v \sim c$ at which the field moves out (Blandford and Znajek 1977; Tchekhovskoy et al. 2010b),

$$P_{\rm jet} \sim (a/M)^2 B^2 r_g^2 c \sim \left(a^2 c/M^2 r_g^2\right)\Phi^2 = k\Phi^2, \tag{4}$$

where the effect of black hole rotation is in the $(a/M)^2$ pre-factor, and the magnetic field is expressed in terms of the flux $\Phi \sim B r_g^2$. Since in the course of an observation M and a usually do not change appreciably, the factor $k = a^2 c/M^2 r_g^2$ is a constant, and all changes in jet power are due to changes in the magnetic flux, Φ.

What is the possible range of Φ and the corresponding range of $P_{\rm jet}$? The lower limit is clear: zero magnetic flux leads to zero power. But what sets the maximum value of Φ? In the simulations of Beckwith et al. (2009) the black hole field strength is comparable to the (mostly gas) pressure in the inner disk, $\beta \sim 1$, suggesting that, in general, equipartition holds. This further suggests that even higher black hole magnetic field strengths are possible for more energetic accretion flows. Tchekhovskoy et al. (2011) carried out numerical simulations of black hole disk-jet systems designed specifically to address the question of maximum field strength. The simulation begins with an initial thick, hot, large scale torus (as shown in Fig. 3(a, b)). Because of the large torus size, it contained a particularly large amount of magnetic flux, much larger than in previous work. Figure 3(a, b) shows the initial condition, compared with initial conditions typically used in previous simulations (Fig. 3(c)). Using these initial conditions Tchekhovskoy et al. (2011) found that magnetic flux on the black hole saturated at an equipartition point, one where the magnetic pressure was sufficient to halt accretion against the inward pull of gravity. In other words, the

Author's personal copy

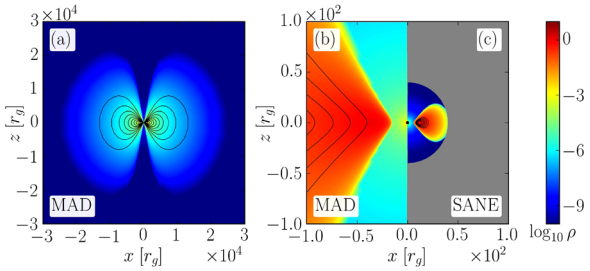

Fig. 3 Panels (**a**) and (**b**) show a meridional slice of density with *color* (*red* shows high, *blue* low density, see *color bar*) and magnetic field lines with *black lines* for the initial conditions of the simulations of Tchekhovskoy et al. (2011) The initial magnetic field is fully contained within the torus, and have a sufficient amount of magnetic flux to saturate the black hole with magnetic flux and to lead to the development of a magnetically-arrested disk (MAD). Panel (**c**) contrasts this initial condition with a typical initial condition in earlier simulations where the torus extent is smaller, and the magnetic flux is reduced. This is labelled "SANE" ICs, for "standard and normal evolution" (Narayan et al. 2012). Figure adapted from Tchekhovskoy (2015)

dynamically-important magnetic flux obstructed the accretion and led to what is dubbed a *magnetically arrested disk*, or a "MAD"; in such a condition no further flux could be carried down to the hole. In contrast, models where magnetic field falls short of saturating the black hole were referred to as "SANE" accretion models, for "standard and normal evolution" by Narayan et al. (2012). In the MAD simulation Φ and $P_{\rm jet}$ are greatly increased, as we discuss below (Tchekhovskoy et al. 2011, 2012; McKinney et al. 2012; Tchekhovskoy 2015).

How do such strong magnetic fields manage to stay in force-balance with the disk? As in previous disk simulations, e.g., Beckwith et al. (2009), the black hole field strength is comparable to the total pressure in the disk. In MADs, magnetic and gas pressures in the disk are comparable, $\beta \sim 1$, but the much stronger black hole magnetic field in the MAD case compresses the inner disk substantially, so the inner regions of MAD disks are actually over-pressured compared to previous simulations by a factor of ~ 5–10.

Figure 4 shows the structure of the simulated disk-jet system. An accretion disk around the central black hole leads to a pair of jets that extend out to much larger distances than the black hole horizon radius and are collimated into small opening angles by outflows from the disk (not shown). Jet magnetic field is predominantly toroidal, which reflects the fact that the jets are produced by the rotation of the black hole, which twists the magnetic field lines into tightly-wound helices.

Even though the accretion disk and the jets turn out to be highly time-variable, in a time-average sense the structure of the flow is remarkably simple. The poloidal magnetic field lines are shown with black solid lines in Fig. 4(b). The group of field lines highlighted in green connects to the black hole and makes up the twin polar jets. As discussed above, these field lines have little to no gas attached to them; disk gas cannot cross magnetic field lines and has too much angular momentum to enter the funnel. The large Poynting flux and very small inertia yields highly relativistic velocities. The field lines highlighted in blue connect to the disk body and make up the magnetic field bundle that produces the slow, heavy disk wind, whose power is much smaller than $P_{\rm jet}$ for rapidly spinning black holes.

The jet power can be characterized by the *outflow energy efficiency* η as

$$\eta = \frac{P_{\rm outflow}}{\dot{M}c^2}. \tag{5}$$

Author's personal copy

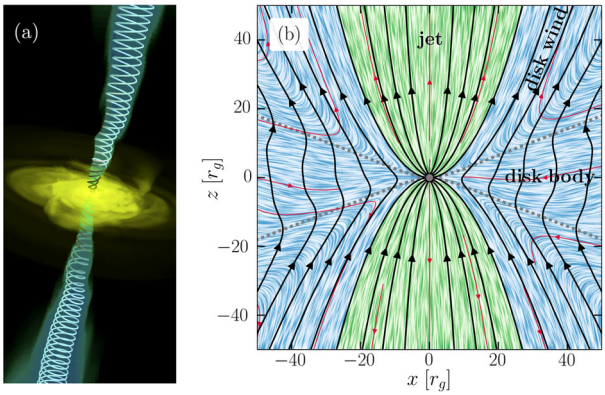

Fig. 4 Panel (**a**): A 3D rendering of a MAD disk-jet simulation. Dynamically-important magnetic fields are twisted by the rotation of a black hole (too small to be seen in the image) at the center of an accretion disk. The azimuthal magnetic field component clearly dominates the jet structure. Density is shown with *color*: disk body is shown with *yellow* and jets with *cyan-blue color*; jet magnetic field lines are *cyan bands*. The image size is approximately $300r_g \times 800r_g$. Panel (**b**): Vertical slice through a MAD disk-jet simulation averaged in time and azimuth. Ordered, dynamically-important magnetic fields remove the angular momentum from the accreting gas even as they obstruct its infall onto a rapidly spinning black hole ($a/M = 0.99$). *Gray filled circle* shows the black hole, *black solid lines* show poloidal magnetic field lines, and *gray dashed lines* indicate density scale height of the accretion flow, which becomes strongly compressed vertically by black hole magnetic field near the event horizon. The symmetry of the time-average magnetic flux surfaces is broken, due to long-term fluctuations in the accretion flow. Streamlines of velocity are depicted both as *thin red lines* and with colored "iron filings", which are better at indicating the fine details of the flow structure. The flow pattern is a standard hourglass shape: equatorial *disk inflow* at low latitudes, which turns around and forms a *disk wind outflow* (labeled as "disk body" and "disk wind", respectively, and highlighted in *blue*), and twin polar *jets* at high latitudes (labeled as "jet" and highlighted in *green*). Figure taken from Tchekhovskoy (2015)

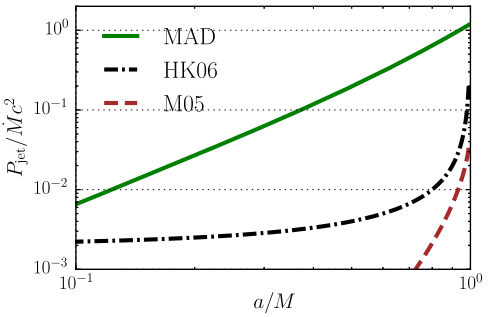

Fig. 5 Comparison of jet energy efficiency obtained in MAD simulations, $P_{\rm jet}/\dot{M}c^2$, which is shown with *green solid line*, with previously reported approximations of simulated jet power: Hawley and Krolik (2006), which is shown with *black dash-dotted line* (HK06), and McKinney (2005), which is shown with *brown dashed line* (M05), plotted over the range $0 \le a/M \le 0.99$. MADs can produce much more powerful jets because they have the maximum possible amount of magnetic flux threading the black hole

For the MAD simulation, the accretion rate $\dot{M}$ fluctuates considerably, but does maintain a well-defined average value. In the MAD flow, for a rapidly spinning black hole, $a/M = 0.99$, the total outflow power, $P_{\rm outflow}$, which is the sum of the black hole powered jet, $P_{\rm jet}$ and the disk powered wind, exceeds the accretion power, $\eta > 1$, i.e., *net* energy is extracted

Author's personal copy

from the black hole (Tchekhovskoy et al. 2011). This is a promising result since high values of jet power are consistent with or are preferred by observations (Rawlings and Saunders 1991; Ghisellini et al. 2010, 2014; Fernandes et al. 2011; McNamara et al. 2011; Nemmen and Tchekhovskoy 2014).

The MAD flow hearkens back to the ion-torus model of Rees et al. (1982) where the role of the thick torus is to confine and anchor the fields that extract rotational energy from the hole, and accretion *per se* is near zero. This model was put originally forward as an explanation for systems where high jet power is seen, but very little luminosity emerges from the central engine. In the MAD flow, accretion continues at a non-zero rate regulated by the magnetic interchange instability in the disk and the strength of the central magnetic field.

Figure 5 compares an analytic approximation for $P_{\rm jet}$ in MAD simulations to some earlier simulations (McKinney 2005; Hawley and Krolik 2006). Jet efficiency in the MAD case is $\propto a^2$, suggesting the ratio of magnetic flux squared to mass accretion rate is roughly constant (Tchekhovskoy et al. 2012; Tchekhovskoy 2015). If MADs achieve the maximum possible amount of magnetic flux threading the black hole then they have achieved the maximum possible jet power for a given mass accretion rate (see Fig. 5). The other models show a rapid rise as a/M approaches 1. Hawley and Krolik (2006) attribute this to greater local field amplification for the extreme Kerr holes; the field has "room to grow," and is a factor of a few smaller than in the MAD simulations.

Efficiencies $\eta > 1$ can lead to spindown of the black hole. For example, in an AGN accreting at 10 % Eddington luminosity, the central black hole is spun down to near-zero spin, $a/M \lesssim 0.1$, in $\tau \simeq 3 \times 10^8$ years (Tchekhovskoy et al. 2012; Tchekhovskoy 2015). This value is interesting astrophysically because it is comparable to a characteristic quasar lifetime (Sect. 5). Over this time period, jets can extract a substantial fraction of the central black hole spin energy and deposit it into the ambient medium. The central galaxy in the cluster MS0735.6+7421 may be one such example (McNamara et al. 2009).

4.2 Origin of the Jet Field

Jets appear to require some large-scale magnetic field, in particular a net vertical field connected either to the disk itself or the central star or black hole. This raises the question of the origin of that field. In the jet-forming global simulations, the initial condition consists of dipole loops embedded within initial orbiting gas, typically a torus of some thickness. In essence, the subsequent evolution (which is a consequence of the initial conditions) transfers the dipole field down to the black hole. Other initial field configurations, such as quadrupolar, toroidal, smaller scale loops, have been found to be far less effective in creating jets (Beckwith et al. 2008).

Simulations that produce jets rely on favorable initial conditions. What happens in Nature? At least two possibilities exist. One is that the required field is generated *in situ* by the disk itself through a dynamo process, as a natural consequence of accretion. Some example dynamo models were discussed above (e.g., Fig. 2). The other possibility is that the required field is carried into the central disk/star, from the companion star in a binary system and from the interstellar medium in an AGN. The advantage of advection is that a relatively weak net field at large radius could be significantly amplified simply by the geometric factor in going from large to small radius. For example, magnetic fields at the edge of the sphere of influence of a supermassive black hole, i.e., $r \sim 100$ pc, are plausibly $B \sim \mu$G. Suppose these fields maintain their coherence over roughly a similar length scale. The magnetic flux contained in patch of field this size, $\Phi_{\rm patch} \approx 10^{35}$ G cm^2, is much larger than the flux

Author's personal copy

necessary to saturate a black hole with magnetic field, $\Phi_{\rm MAD} \approx 10^{33.5}$ G cm^2 (for a black hole of mass $M = 10^9 M_\odot$ accreting at 10 % of Eddington luminosity, Narayan et al. 2003; Tchekhovskoy 2015).

Under what general circumstances can a net field be advected in by the accretion flow? The question is traditionally framed in the terms used by van Ballegooijen (1989), namely that accretion rate is set by the viscosity ν and the magnetic diffusion by the resistivity η. Whether or not a field can be advected inward depends on the magnetic Prandtl number $P_m = \nu/\eta$. If P_m exceeds 1 then field advection will not occur (see also Lubow et al. 1994). In accretion disks the viscosity and resistivity are not the physical values, but instead are effective values resulting from the turbulence (Guan and Gammie 2009; Lesur and Longaretti 2009; Fromang and Stone 2009).

In global simulations, flux in the initial torus (e.g. Fig. 5) finds its way onto the black hole, despite starting from a large radius. This suggests that geometrically-thick disks are capable of transporting large-scale magnetic flux inward, at least from the distances of $r \sim 100 r_g$. In standard α-disk theory, infall rates are proportional to $(h/r)^2$. If h/r is close to unity the infall time becomes relatively rapid, and the inflow rate can exceed the diffusion rate. Thick, radiatively inefficient flows, then, seem to have the best chance of transporting flux inward.

The question of whether a turbulent, radiatively efficient disk could transport flux inward remains an interesting one. Beckwith et al. (2009) studied the question through a global simulation of an initial orbiting torus with an $h/r \sim 0.1$ embedded in a vertical magnetic field. They found that there was no net flux transported through the disk itself; the turbulence transported angular momentum and mass, but not net flux. Net flux was nevertheless brought down to the black hole by a coronal inflow surrounding the accretion disk. Initially the field lies along cylinders of constant rotation, but at high altitude B^2/ρ is much larger than deep inside the disk, and the field is subject to a finite-amplitude version of the MRI. The sign relation between the radial field component and the toroidal field component is the usual one, so the Maxwell stress has the right sign to transport angular momentum outward. The angular momentum flux due to the Maxwell stress is large compared to the fluid angular momentum density. Fluid elements at high altitude, both above and below the equator, are therefore driven inward quickly, carrying half-loops of field with them. When one loop approaches the central black hole from above and outward while another approaches the disk from below and outward, their local field directions are opposed, and they can reconnect. Reconnection changes the field topology, creating a closed loop at larger radius and an open field line at small radius. The open field line, the one carrying the net flux, is located where the reconnection occurred, which is at a radius considerably smaller than the initial radius of the field line. Thus, reconnection causes the flux to move inward in large jumps. All of this takes place faster than the mean mass inflow rate within the disk at the vicinity of the flux line's initial position.

In a similar vein, Suzuki and Inutsuka (2014) carried out a series of simulations with a relatively thick disk (sound speed ~ 0.1 of the orbital speed) with an initial weak magnetic field. In these simulations net vertical flux was carried inward by a rapidly infalling layer near the disks surface. All these simulations transport net flux through a mechanism that is governed by large-scale torques and resulting rapid inflows, rather than by small-scale turbulence where the turbulent velocities exceed the mean inward drift velocity associated with accretion. It appears plausible, therefore, that net inward flux transport can occur for certain types of accretion flows.

Testing jet-generation models, including quantitative predictions for the magnetic flux close to the black hole, fundamentally depends on observations that can give insights into the field properties both at the jet base and further out. We discuss those in the following section.

Author's personal copy

5 Observational Constraints on Jet Magnetic Fields

5.1 Introduction: Basic Jet Properties

In this section we ask what the observational constraints are on the field strengths and configurations in jets, and whether these observational results can be connected to jet-launching models. (For a more detailed review of these issues see Pudritz et al. 2012; parts of that work are summarized in this section.) We focus on relativistic AGN jets, since these are by far the best-studied of the systems producing synchrotron radiation, and begin by setting out some basic properties of the jets in radio-loud AGN.

AGN jets are fast outflows carrying kinetic powers that are estimated to be between $\sim 10^{42}$ and $\sim 10^{47}$ erg s^{-1} (e.g., Rawlings and Saunders 1991). Bulk speeds are known to be highly relativistic on small scales ($\Gamma \sim 10$–30, and perhaps higher in some objects: Lister et al. 2009); on kpc scales some jets have decelerated to sub-relativistic speeds (Laing and Bridle 2002) while in more powerful systems jets are at least mildly relativistic out to hundred-kpc scales (Mullin and Hardcastle 2009) and may retain a highly relativistic spine with $\Gamma \sim 10$ out to those scales, though direct observational evidence for this remains debatable (e.g., Tavecchio et al. 2000; Hardcastle 2006; Marshall et al. 2011; Konar and Hardcastle 2013).

Jet composition remains an open question. Observations of synchrotron radiation require relativistic leptons and magnetic fields to be present, but *direct* observational constraints on the presence of a hadronic component are hard to obtain. Some indirect constraints suggest that the bulk of the required energy for jets can be carried by the radiating leptons without any need for additional components on scales from pc to kpc (e.g., Wardle et al. 1998; Croston et al. 2005; Wykes et al. 2013), it is certain that all jets must entrain material from stellar winds in the host galaxy (Bicknell 1994) so their composition may change with distance along the jet, and there is some evidence from pressure balance arguments that this is indeed the case (Croston and Hardcastle 2014).

One important observational constraint on jet launching mechanisms comes from the fact that they appear to be able to originate in AGN with a wide range of different properties. The vast majority of radio-loud AGN are so-called 'low-excitation radio galaxies' which show no evidence at any wavelength for a standard radiatively efficient accretion disk (Hardcastle et al. 2009; Best and Heckman 2012). However, the existence of powerful radio-loud quasars with $L/L_{\rm Edd} \sim 1$ in the optical shows that radiatively inefficient accretion is not directly connected to radio jet activity. In fact it appears that radio-loud AGN have a very wide range of $L/L_{\rm Edd}$, even when jet power is taken into account (Mingo et al. 2014).

Finally, it is important to note that observations of synchrotron radiation require a particle acceleration mechanism. There is indirect or direct evidence for local particle acceleration on all scales of radio-loud AGN up to scales of tens of kpc. Shocks are almost certainly implicated—some of the best-understood sites of particle acceleration, the hotspots of powerful double radio galaxies, are clearly physically associated with the jet-termination shock and show properties consistent with simple first-order Fermi acceleration (Meisenheimer et al. 1997). However, other mechanisms may well be necessary to explain diffuse particle acceleration distributed on scales of many kpc (e.g., Hardcastle et al. 2007). When interpreting observations, it is necessary to bear in mind that the particles being observed at a given location may owe their energy spectrum to acceleration in some region that is spatially quite distinct.

Because jets can be persistent (ages of the order 10^8 years have been estimated for some sources based on spectral or dynamical age estimates) they produce large-scale, long-lasting

Author's personal copy

structures consisting of material that has passed up the relativistic jet (Scheuer 1974), generally called lobes or plumes. The physical conditions in these structures are to some extent determined by the jet and so they give important clues to aspects of the jets that are hard to investigate directly. Because the observational techniques used are rather different, it is usual to discuss the large-scale lobes, the kpc-scale jets and the pc-scale jets separately, a convention that we follow in the remainder of this section.

5.2 Observational Tools

The combination of relativistic leptons and magnetic field gives rise to synchrotron emission, while relativistic leptons and a photon field give us inverse-Compton emission. These are the basic tools available to estimate the magnetic field properties in jets and their products.

Optically thin synchrotron radiation cannot on its own give a measurement of magnetic field strength. For simplicity, let us represent the electron energy spectrum as a power law with index p, so that $N(E) = N_0 E^{-p}$. Then the synchrotron emissivity in the optically thin regime is given by

$$J(\nu) = C N_0 \nu^{-\frac{(p-1)}{2}} B^{\frac{(p+1)}{2}} \tag{6}$$

where C is a constant depending only weakly on p. Equation (6) implies that the same observed emissivity can be produced by any combination of the number density of electrons (scaling as N_0) and the strength of the field B. However, total intensity emission does give important information about the magnitude of any spatial *variation* in field strength (combined with electron density, energy spectrum etc) given the strong dependence on B of emissivity (Eq. (6)). The direction of observed polarization in optically thin regions gives us an (emission-weighted, line-of-sight integrated, projected) estimate of the local direction of magnetic field, which is our best probe of the vector properties of the field, while fractional polarization tells us about its ordering: for a uniform field the fractional polarization for power-law electron energy index p is $\Pi = (p+1)/(p+\frac{7}{3})$.

Faraday rotation can complicate the interpretation of polarization. For the simple case of an external Faraday screen, the rotation angle ϕ is given by

$$\phi = \frac{c^2}{\nu^2} K \int_0^s n_{\rm th} \mathbf{B}.\mathrm{d}\mathbf{s} \tag{7}$$

where K is a constant, $n_{\rm th}$ is the number density of thermal electrons, and the integral is along the line of sight to the source. If the value of ϕ varies within the resolution element, depolarization rather than simple rotation with $\phi \propto \lambda^2$ will be observed. In some cases, therefore polarized intensity, and in particular the dependence of fractional polarization or position angle on frequency, actually tells us more about the foreground magnetoionic medium (in the host or the Milky Way) than it does about the source itself. The effects of internal and external Faraday-active media on polarization are well understood in some simple analytic cases (Burn 1966; Jones and O'Dell 1977; Cioffi and Jones 1980).

Optically thick synchrotron radiation is an essential tool for field strength measurements on the pc scale; the turnover frequency for synchrotron self-absorption is sensitively dependent on the magnetic field strength, with the absorption coefficient going as $B^{(p+2)/2}$. However, as the turnover also depends on the normalization of the electron energy spectrum, this method depends on good information about the structure of the components where the turnover is observed.

Author's personal copy

The combination of inverse-Compton and synchrotron emission gives an excellent constraint on the mean field strength, if both processes can be measured from the same region; inverse-Compton emissivity depends only on the number density of electrons (for a known photon field, often the CMB) so that the field strength may be directly estimated from the synchrotron emissivity. Again, it is necessary to know the geometry of the emitting region accurately,

Finally, if all else fails, it is traditional to resort to the assumptions of equipartition,

$$\frac{B^2}{8\pi} = \int EN(E)\mathrm{d}E \tag{8}$$

or minimum energy (Burbidge 1956)

$$U_{\mathrm{tot}} = \frac{B^2}{8\pi} + \int EN(E)\mathrm{d}E: \quad \frac{\mathrm{d}U_{\mathrm{tot}}}{\mathrm{d}B} = 0 \tag{9}$$

which, putting in B-dependent estimates of N_0 from Eq. (6), give fairly similar magnetic field values for a given volume emissivity. Until recently there has been little observational justification for the equipartition assumption (though see below) and it should still be applied with caution.

5.3 Observations: Large-Scale Components

In the large-scale lobes and plumes of radio galaxies the gold standard for field strength measurements is the inverse-Compton technique. Large numbers of powerful (FRII: Fanaroff and Riley 1974) radio galaxies now have global lobe field strength measurements (Kataoka and Stawarz 2005; Croston et al. 2005) using X-ray inverse-Compton measurements made with *XMM* and *Chandra*. These imply field strengths close to, but somewhat below, the equipartition values: a typical field strength in a lobe is of the order 10 μG. Fewer such measurements exist for the lower-power FRI radio galaxies, in part because of their typically brighter thermal environments but also because some part of their internal pressure is probably provided by thermal material (Hardcastle and Croston 2010). However, a magnetic field strength around 1 μG, again close to the equipartition value, has been estimated for the nearby FRI radio galaxy Centaurus A based on *Fermi* γ-ray detections of its large-scale lobes (Abdo et al. 2010).

Inverse-Compton observations also provide important evidence for the spatial intermittency of the magnetic field: the inverse-Compton surface brightness (which, for scattering of the CMB, depends only on the electron energy density and the line-of-sight depth) is seen to be much more uniform than the synchrotron surface brightness (Hardcastle and Croston 2005). This is as expected if the lobes are turbulent with an energetically sub-dominant magnetic field, and similar effects are seen in numerical MHD modeling of lobes (Tregillis et al. 2004; Hardcastle and Krause 2014).

Turning to field direction, the apparent field directions inferred from polarization measurements in the lobes are almost always perpendicular to the jet far away from the jet termination, with mean fractional polarization in the range 20–40 % at high frequencies. This is consistent with the idea that a toroidal component of the field dominates on large scales, as would be expected if an initially disordered field expands into the lobes, but compression of a disordered field can give similar results (Laing 1980).

Author's personal copy

5.4 Observations: kpc-Scale Jets and Termination Features

Inverse-Compton measurements of field strengths in jets are difficult because of the existence of *in situ* particle acceleration, which can give rise to high-energy (e.g. X-ray) synchrotron emission. Arguments for high bulk speeds in kpc-scale jets, discussed above, assume that the X-ray emission from these jets is synchrotron, but there is a degeneracy between the magnetic field strength and the (a priori unknown) jet speed and angle to the line of sight, so that these observations are not very useful for measurements. In low-power jets, where the dynamics are better understood, TeV γ-ray observations place some constraints on magnetic field strength (Hardcastle and Croston 2011), implying $B > 20$ μG to avoid over-producing the observed TeV emission. These models depend on a good knowledge of the photon field, in this case the starlight at the centre of the elliptical host galaxy.

The magnetic field direction is much better understood. In powerful jets the field direction is almost universally along the jet (although it is not clear whether the synchrotron emission from the jet is a reliable tracer of the jet itself—it may simply show a boundary layer). In low-power jets, observations of polarization are essential to models that break the degeneracy between jet speed and angle to the line of sight (Laing and Bridle 2002) and when this is done it is found that the field tends to evolve from a predominantly longitudinal configuration on the smallest scale to a predominantly toroidal one after jet deceleration: no significant radial component is required by the models (Laing and Bridle 2014). Helical field models on these scales for these well-studied low-power jets are ruled out by the lack of transverse polarization asymmetry.

Powerful jets terminate in compact (1–10 kpc scale), bright features known as hotspots, which are thought to trace the jet termination shock. As the downstream material should be subsonic, and so at most mildly relativistic, hotspots are easier to understand than the jets themselves. Their brightness means that they are good sources of inverse-Compton emission via the synchrotron self-Compton process, producing X-ray emission (Harris et al. 1994). Inverse-Compton modeling implies field strengths of the order 100 μG in hotspots of powerful sources (Hardcastle et al. 2004; Kataoka and Stawarz 2005). Magnetic field structures in hotspots, as revealed by high-resolution polarization imaging, are complex, but there is a general tendency for the projected field direction to be perpendicular to the jet (Leahy et al. 1997).

5.5 Observations: pc-Scale Jets

Inverse-Compton methods are very uncertain on small scales—high-energy emission from the jet is often hard to distinguish from emission from other components of AGN. In objects where this is not the case, such as blazars, the jet geometry, bulk speed and angle to the line of sight are likely to be poorly known. Most methods for estimating the magnetic field strength on parsec scales rely on inferences from very long baseline interferometry (VLBI) in the radio, and hence on synchrotron emission. Typically, the parsec-scale radio morphology of a bright AGN manifests a one-sided jet structure due to Doppler boosting, which enhances the emission of the approaching jet. As noted above, Lorentz factors on these scales can be high, $\Gamma \sim 10$–30: constraints come from observations of apparent motions (Cohen et al. 2007; Lister et al. 2013) and from radio variability (Jorstad et al. 2005; Hovatta et al. 2009; Savolainen et al. 2010).

The apparent base of the jet, which is often the brightest and least-resolved part, is commonly called the *core*. As noted above, synchrotron self-absorption, which depends on both the particle number density N_e and the magnetic field B, will affect the appearance of the jet; the core is thought to represent the jet region where the optical depth is

Author's personal copy

equal to unity. As the number density and magnetic field depend on distance from the jet base, the position of the apparent core is expected to depend on observing frequency. This is the basis of the *core-shift* method for estimating magnetic field strengths (Lobanov 1998; O'Sullivan and Gabuzda 2009b), evaluating the relation between core flux at given frequency and mass of black hole (Heinz and Sunyaev 2003), jet composition (Hirotani 2005), and flow magnetization (Nokhrina et al. 2015). This method necessarily assumes that the jet is well described by the simple, homogeneous conical jet models of Blandford and Königl (1979). The latter assumption is supported by multi-frequency observations by Sokolovsky et al. (2011).

As an alternative to the core-shift method, individual components of the jet can be fitted with self-absorption models (e.g. Savolainen et al. 2008); this method is less model-dependent but has larger random errors as a result of the uncertainties on component size, geometry and Doppler factor. Magnetic field strengths derived by either method are of the order 1 G on pc scales. Recently, Zdziarski et al. (2015) have proposed a "hybrid" method of doing core-shift analysis which does not rely on the equipartition assumption, again obtaining similar magnetic field strength values.

On pc scales, the inferred jet magnetic field direction is normally either parallel or perpendicular to the jet direction (e.g. Lister and Homan 2005), with jets in more powerful objects tending to have parallel fields. Misaligned polarization that is definitively not the result of Faraday rotation is rare. The interpretation of these field structures varies: they are often attributed to internal jet dynamics, e.g. shocks in the case of transverse apparent field direction, but could equally well be the result of an underlying helical magnetic field geometry with varying pitch angle (Lyutikov et al. 2005). (As noted above, helical fields are expected in most jet generation models due to the toroidal component introduced by field winding: see Sects. 1, 4.2.) As pointed out by Blandford (1993), the helical-field model would be supported by observations of transverse gradients of Faraday rotation across the jet, provided that there are thermal electrons in the jet or in its immediate environment to provide the required magnetoionic medium (Eq. (7)). Detection of such gradients is observationally difficult, since the jets are poorly resolved, but they have been observed in a number of objects (e.g., Asada et al. 2002; O'Sullivan and Gabuzda 2009a; Croke et al. 2010). While their interpretation is still controversial (Taylor and Zavala 2010) these gradients provide at least some direct evidence for helical field structures in the inner parts of the jets.

5.6 Core-Shifts and Jet Magnetization

Two important MHD parameters for describing relativistic flows are the Michel magnetization parameter $\sigma_{\rm M}$ and the multiplicity parameter λ. The first one tells us how strongly the flow is magnetized at its origin, and it determines the maximum possible bulk Lorentz factor of the flow. The second one is the dimensionless multiplicity parameter $\lambda = N_{\rm e}/N_{\rm GJ}$, which is defined as the ratio of the number density $N_{\rm e}$ to the Goldreich-Julian (GJ) number density $N_{\rm GJ} = \Omega B/2\pi ce$—the minimum number density needed for screening the longitudinal electric field. These two parameters are connected with total jet power $P_{\rm jet}$ by equation (Beskin 2010)

$$\sigma_{\rm M} \approx \frac{1}{\lambda}\left(\frac{P_{\rm jet}}{P_{\rm A}}\right)^{1/2}. \tag{10}$$

Here $P_{\rm A} = m_{\rm e}^2 c^5/e^2 \approx 10^{17}$ erg/s is the minimum energy loss rate of a central engine which can accelerate particles to relativistic energies.

Author's personal copy

There are two theoretical models of plasma production in a jet. In the first one, pairs are produced by two-photon collisions with photons with sufficient energy produced by the inner parts of the accretion disk (Blandford and Znajek 1977). In this case we expect $\lambda \sim 10^{10}$–10^{13}, and Michel magnetization parameter $\sigma_{\rm M} \sim 10$–10^3. The second model of the pair production is a cascade process in non-zero electric field in a region with the zero GJ plasma density due to general relativity effects (Beskin et al. 1992; Hirotani and Okamoto 1998). This model gives $\lambda \sim 10^2$–10^3, and magnetization $\sigma_{\rm M} \sim 10^{10}$–$10^{13}$. So in both scenarios the flow is strongly magnetized at its base, but this large difference in the estimates for the magnetization parameter $\sigma_{\rm M}$ leads to two different pictures of the flow structure in jets. Indeed, as has been shown by several authors (Beskin and Nokhrina 2006; Tchekhovskoy et al. 2009; Komissarov et al. 2009), for well-collimated magnetically dominated MHD jets the Lorentz factors of the particle bulk motion follows the relation

$$\Gamma \approx r_\perp / R_{\rm L}, \tag{11}$$

where $r_\perp$ is the distance from the jet axis, and $R_{\rm L} = c/\Omega$ is the light cylinder radius. The relation (11) holds until the flow reaches the equipartition regime—the Poynting flux is approximately equal to the particle kinetic energy flux. Further acceleration is ineffective. For ordinary jets $r_\perp / R_{\rm L} \sim 10^4$–$10^5$. As a result, using the universal asymptotic solution (11), one can find that values $\sigma_{\rm M} \sim 100$ correspond to the saturation regime when there is approximately equipartition between the Poynting flux $P_{\rm em}$ and the particle kinetic energy flux $P_{\rm part}$. On the other hand, for $\sigma_{\rm M} \sim 10^{12}$ the jet remains magnetically dominated ($P_{\rm part} \ll P_{\rm em}$). Thus, the determination of the Michel magnetization parameter $\sigma_{\rm M}$ is a key point in the analysis of the internal structure of relativistic jets.

The core-shift measurements described above (Gould 1979; Marscher 1983; Sokolovsky et al. 2011; Pushkarev et al. 2012) might provide an observational way to probe λ and $\sigma_{\rm M}$. The ideal MHD flow of plasma with exactly the drift velocity in crossed electric and magnetic fields does not emit synchrotron radiation. However, some internal dissipative processes, for example internal shocks and magnetic reconnection, can produce particles with a non-thermal spectrum that can account for the observed emission. By measuring the core-shift discussed in the previous subsection, one can obtain the combination of magnetic field magnitude $B_{\rm cs}$ and electron number density $N_{\rm cs}$ in the region with optical depth equal to unity. On the other hand, $B_{\rm cs}$ and $N_{\rm cs}$ can be related through the flow magnetization $\sigma = \sigma_{\rm M}/\Gamma - 1$ (Tchekhovskoy et al. 2009) assuming that the flow is in the saturation regime, i.e. $\sigma_{\rm cs} \approx \sigma_{\rm M}/2 \approx \Gamma_{\rm cs}$ (Beskin and Nokhrina 2006; Tchekhovskoy et al. 2009; Komissarov et al. 2009). Combining the latter with the definitions of λ and $\sigma_{\rm M}$, one can obtain both λ and $\sigma_{\rm M}$ as a function of core-shift and total jet power $P_{\rm jet}$. The latter can be estimated by correlating the radio jet luminosity to total power needed to form the cavities in surrounding gas (Cavagnolo et al. 2010). This analysis leads to estimates of $\lambda \sim 10^{13}$ and $\sigma \sim 10$ (Nokhrina et al. 2015). The measurements of core-shift by Pushkarev et al. (2012) thus allow the order of Michel magnetization at the jet base to be estimated, and it can be concluded that the MHD flow on the observable scales are in the saturation regime, i.e. there is no effective plasma acceleration by the MHD mechanism downstream. Moreover, the order of $\sigma_{\rm M}$ correlates well with the estimated Lorentz factors of jet flows discussed above.

Recently, it has become possible to use the core-shift to measure the magnetic flux threading the jets and central black holes in a rather large sample of radio-loud active galactic nuclei (Zamaninasab et al. 2014; Zdziarski et al. 2015). Dynamically-important black hole magnetic fields were inferred, indicating that the central black holes of most if not all radio-loud AGN are in a MAD state (Sect. 4.2). MADs have also been inferred in tidal disruption events (Tchekhovskoy et al. 2014) and core-collapse gamma-ray bursts (Tchekhovskoy and

Author's personal copy

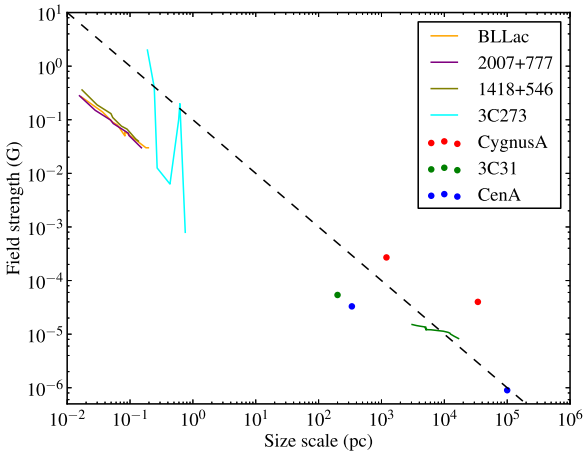

Fig. 6 Magnetic field strengths on different size scales illustrated using a few well-studied objects on pc and kpc scales. The size scale plotted here is the transverse radius of the component in which the field is measured, not the distance from the nucleus (though in general the two scale). Data are taken from O'Sullivan and Gabuzda (2009b), Savolainen et al. (2008), Hardcastle et al. (2004), Hardcastle and Croston (2010, 2011), Croston and Hardcastle (2014), and Abdo et al. (2010). The *solid line* shows an arbitrarily normalized line of $B \propto r^{-1}$—we would expect the normalization of this line to depend on the jet power so it is not surprising that all points do not lie on the line

Giannios 2014). This suggests that MADs are perhaps not rare or unusual as their name might imply, but possibly quite the opposite.

5.7 Observational Summary

To summarize, we now have relatively good information about the magnetic field strengths on kpc scales, and excellent information about the vector properties of the field, which, however, are probably not strongly connected to the field properties at jet generation. On pc scales and below, magnetic field strengths are not as well constrained, but such constraints from, e.g., core-shift observations as we have are consistent with the expectations from models, while polarization observations are certainly consistent with the presence of a helical field structure on small scales.

The field strength constraints obtained for some of the objects discussed above are summarized in Fig. 6, which shows a broad consistency with an r^{-1} scaling over the observable ~ 7 orders of magnitude in physical scale. Fields of the order 10^4 G, and thus magnetic fluxes $\sim 10^{33}$ G cm^2 would be implied by an extrapolation to scales comparable to the gravitational radius of the central black hole. In principle, magnetic fluxes at this level could be dynamically important (plasma $\beta \sim 1$) and so could affect the flow of material in the disk as discussed in Sect. 4.2.

6 Conclusions

Accretion disks and the jets they produce are fundamentally magnetic systems. A great deal of progress has been made in the theory of these systems, and in obtaining their properties from observation. We began by considering how the entire complex system is broken into

Author's personal copy

different components for theoretical analysis. Where then do we stand with those components?

First, accretion disks are turbulent, and that turbulence is almost certainly created by the instability to the MRI. This MRI-induced turbulence produces internal stress that can transport angular momentum at the rates required.

Although it seems clear that disks are magnetic, jets appear to require a more organized magnetic field than is produced by MRI turbulence. The origin of the jet magnetic field remains uncertain. A disk dynamo remains a possibility, and dynamo action has been seen in some simulations, but the field produced is not the type required for jet launching. In the case of stellar jets, the central star may also be the source of the required field through its own internal dynamo. The possibility remains that the required field could be carried in from large radii; however, MRI turbulence does not seem to accomplish that on its own. More direct infall, taking place outside the turbulent disk proper, or in a hot, thick accretion flow with relatively large infall velocities, could work if the resulting field is able to reconnect as needed to establish the required topology on the central star or black hole, or through the central accretion disk.

The general model of jets as magnetized, accelerated and collimated disk winds is well established today by observations and theoretical investigations. While for young stars the disk wind seems to play the major role in jet launching (Blandford-Payne), the jets from AGN and other relativistic sources are plausibly dominated by processes energetically supported directly by the spinning black hole (Blandford-Znajek, Blandford and Znajek 1977), and observations, at least on the smallest scales, show good consistency with the expectations of this type of model, as discussed in Sect. 5. There are still many unknowns. For example, the matter content of relativistic jets is as yet unclear, and in many cases their propagation speed is poorly constrained; there is no direct measurement of the magnetic field of jets from stars or of the accretion disk.

Global MHD simulations are able to treat the global jet launching that is the accretion-ejection process. Usually an initial large-scale magnetic field has been assumed so far in these models, only a few simulations were able to consider mean-field disk dynamo. How such global, axisymmetric mean-field models match the disk microphysics and the respective local disk simulations, is still an open question. The magnetized disks considered in jet launching simulations use a rather simple model for the (turbulent) magnetic diffusivity or viscosity and also neglect radiation and radiative transport processes. However, all these processes seem to be essential for the disk physics.

Future progress will clearly come from more sophisticated simulation models, considering the physical effects mentioned above. The codes and computational resources may not yet be ready for such an ambitious goal, as the treatment of the additional physics will require new numerical methods, and also a higher numerical resolution, together with a fully 3D treatment.

Simulations have clearly demonstrated the viability of the Blandford-Znajek type jet powered by a rotating black hole. Those simulations further suggest that a dipole field is required, in addition to the rotating hole, and that the field strength is set by equipartition with the surrounding pressure (gas, ram, magnetic) associated with the accretion disk. The issue of the presence of such jets comes back to the origin of the axial black hole field, a problem that remains uncertain, as discussed above.

Finally, we have seen that observations, particularly of AGN jets, are starting to provide direct tests of jet-launching models through constraints on the bulk speed, particle content, kinetic power, and magnetic field strength and configuration of jets. Much progress on at least some of these issues can be expected from the improvement in observational

Author's personal copy

capabilities at arcsecond resolutions (and thus generally kpc scales) to be provided by next-generation radio facilities such as the upgraded JVLA and LOFAR, and in the future the SKA. However, the most direct constraints remain those provided by long-baseline interferometers such as the VLBA and EVN, and continued support of these is vital if we are to be able to make direct tests of jet models in the future.

Acknowledgements The authors would like to thank the ISSI team for their support and hospitality, and for the organization of a great workshop and fruitful discussions during the week in Bern. This work was also supported by NSF grant AST0908869 (JFH) and by funding from the UK STFC (MJH). AT was supported by NASA through Einstein Postdoctoral Fellowship grant number PF3-140115 awarded by the *Chandra* X-ray Center, which is operated by the Smithsonian Astrophysical Observatory for NASA under contract NAS8-03060, and NASA via High-End Computing (HEC) Program through the NASA Advanced Supercomputing (NAS) Division at Ames Research Center that provided access to the Pleiades supercomputer, as well as NSF through an XSEDE computational time allocation TG-AST100040 on NICS Kraken, Nautilus, TACC Stampede, Maverick, and Ranch. AT used Enthought Canopy Python distribution to generate the figures for this work. JFH wishes to thank Julian Krolik for useful discussions.

References

A.A. Abdo et al., Science **328**, 725 (2010)
J.M. Anderson, Z.-Y. Li, R. Krasnopolsky, R.D. Blandford, Astrophys. J. **630**, 945 (2005)
K. Asada et al., Proc. Astron. Soc. Jpn. **54**, L39 (2002)
M. Avila, Phys. Rev. Lett. **108**, 124501 (2012)
X.-N. Bai, J.M. Stone, Astrophys. J. **767**, 30 (2013a)
X.-N. Bai, J.M. Stone, Astrophys. J. **769**, 76 (2013b)
S.A. Balbus, J.F. Hawley, Astrophys. J. **376**, 214 (1991)
S.A. Balbus, J.F. Hawley, Rev. Mod. Phys. **70**, 1 (1998)
S.A. Balbus, J.C.B. Papaloizou, Astrophys. J. **521**, 650 (1990)
S.A. Balbus, J.F. Hawley, J.M. Stone, Astrophys. J. **467**, 76 (1996)
K.R.C. Beckwith, J.F. Hawley, J.H. Krolik, Astrophys. J. **678**, 1180 (2008)
K.R.C. Beckwith, J.F. Hawley, J.H. Krolik, Astrophys. J. **707**, 428 (2009)
V.S. Beskin, Phys. Usp. **53**, 1199 (2010)
V.S. Beskin, E.E. Nokhrina, Mon. Not. R. Astron. Soc. **367**, 375 (2006)
V.S. Beskin, Ya.N. Istomin, V.I. Pariev, Sov. Astron. **36**, 642 (1992)
P.N. Best, T.M. Heckman, Mon. Not. R. Astron. Soc. **421**, 1569 (2012)
G.V. Bicknell, Astrophys. J. **422**, 542 (1994)
R.D. Blandford, Astrophys. Space Sci. Libr. **103**, 15 (1993)
R.D. Blandford, A. Königl, Astrophys. J. **232**, 34 (1979)
R.D. Blandford, D.G. Payne, Mon. Not. R. Astron. Soc. **199**, 883 (1982)
R.D. Blandford, R.L. Znajek, Mon. Not. R. Astron. Soc. **179**, 433 (1977)
A. Brandenburg, A. Nordlund, R.F. Stein, U. Torkelsson, Astrophys. J. **446**, 741 (1995)
G. Burbidge, Astrophys. J. **124**, 416 (1956)
B.J. Burn, Mon. Not. R. Astron. Soc. **133**, 67 (1966)
C. Carrasco-González, L.F. Rodríguez, G. Anglada, J. Martí, J.M. Torrelles, M. Osorio, Science **179**, 433 (2010)
F. Casse, J. Ferreira, Astron. Astrophys. **361**, 1178 (2000)
F. Casse, R. Keppens, Astrophys. J. **581**, 988 (2002)
F. Casse, R. Keppens, Astrophys. J. **601**, 90 (2004)
K.W. Cavagnolo, B.R. McNamara, P.E.J. Nulsen et al., Astrophys. J. **720**, 1066 (2010)
D.F. Cioffi, T.W. Jones, Astron. J. **85**, 368 (1980)
M.H. Cohen et al., Astrophys. J. **658**, 232 (2007)
J. Contopoulos, R.V.E. Lovelace, Astrophys. J. **429**, 139 (1994a)
J. Contopoulos, Astrophys. J. **432**, 508 (1994b)
S.M. Croke, S.P. O'Sullivan, D.C. Gabuzda, Mon. Not. R. Astron. Soc. **402**, 259 (2010)
J.H. Croston, M.J. Hardcastle, Mon. Not. R. Astron. Soc. **438**, 3310 (2014)
J.H. Croston et al., Astrophys. J. **626**, 733 (2005)
J.-P. De Villiers, J.F. Hawley, J.H. Krolik, S. Hirose, Astrophys. J. **620**, 878 (2005)
J.-F. Donati, F. Paletou, J. Bouvier, J. Ferreira, Nature **438**, 466 (2005)

Author's personal copy

E.M. Edlund, H. Ji, Phys. Rev. E **89**, 021004 (2014)
B.L. Fanaroff, J.M. Riley, Mon. Not. R. Astron. Soc. **167**, 31P (1974)
Ch. Fendt, Astrophys. J. **651**, 272 (2006)
Ch. Fendt, Astrophys. J. **692**, 346 (2009)
Ch. Fendt, M. Cemeljic, Astron. Astrophys. **334**, 750 (1998)
Ch. Fendt, M. Cemeljic, Astron. Astrophys. **395**, 1045 (2002)
Ch. Fendt, S. Sheikhnezami, Astrophys. J. **774**, 12 (2013)
Ch. Fendt, M. Camenzind, S. Appl, Astron. Astrophys. **300**, 791 (1995)
C.A.C. Fernandes, M.J. Jarvis, S. Rawlings et al., Mon. Not. R. Astron. Soc. **411**, 1909 (2011)
J. Ferreira, Astron. Astrophys. **319**, 340 (1997)
J. Ferreira, G. Pelletier, Astron. Astrophys. **276**, 625 (1993)
A. Frank et al., in *Protostars and Planets VI*, ed. by H. Beuther, R.S. Klessen, C.P. Dullemond, T. Henning (University of Arizona Press, Tucson, 2014)
S. Fromang, J.M. Stone, Astron. Astrophys. **507**, 19 (2009)
C.F. Gammie, S.L. Shapiro, J.C. McKinney, Astrophys. J. **602**, 312 (2004)
G. Ghisellini, F. Tavecchio, L. Foschini et al., Mon. Not. R. Astron. Soc. **402**, 497 (2010)
G. Ghisellini, F. Tavecchio, L. Maraschi, A. Celotti, T. Sbarrato, Nature **515**, 376 (2014)
R.J. Gould, Astron. Astrophys. **76**, 306 (1979)
O. Gressel, Mon. Not. R. Astron. Soc. **405**, 41 (2010)
X. Guan, C.F. Gammie, Astrophys. J. **697**, 1901 (2009)
X. Guan, C.F. Gammie, Astrophys. J. **728**, 130 (2011)
M.J. Hardcastle, Mon. Not. R. Astron. Soc. **366**, 1465 (2006)
M.J. Hardcastle, J.H. Croston, Mon. Not. R. Astron. Soc. **363**, 649 (2005)
M.J. Hardcastle, J.H. Croston, Mon. Not. R. Astron. Soc. **404**, 2018 (2010)
M.J. Hardcastle, J.H. Croston, Mon. Not. R. Astron. Soc. **415**, 133 (2011)
M.J. Hardcastle, M.G. Krause, Mon. Not. R. Astron. Soc. **443**, 1482 (2014)
M.J. Hardcastle, D.E. Harris, D.M. Worrall, M. Birkinshaw, Astrophys. J. **612**, 729 (2004)
M.J. Hardcastle, J.H. Croston, R.P. Kraft, Astrophys. J. **669**, 893 (2007)
M.J. Hardcastle, D.A. Evans, J.H. Croston, Mon. Not. R. Astron. Soc. **396**, 1929 (2009)
D.E. Harris, C.L. Carilli, R.A. Perley, Nature **367**, 713 (1994)
J.F. Hawley, Astrophys. J. **528**, 462 (2000)
J.F. Hawley, S.A. Balbus, Astrophys. J. **573**, 738 (2002)
J.F. Hawley, J.H. Krolik, Astrophys. J. **641**, 103 (2006)
J.F. Hawley, C.F. Gammie, S.A. Balbus, Astrophys. J. **440**, 742 (1995)
J.F. Hawley, C.F. Gammie, S.A. Balbus, Astrophys. J. **464**, 690 (1996)
S. Heinz, R. Sunyaev, Mon. Not. R. Astron. Soc. **343**, L59–L64 (2003)
J.J. Hester, K. Mori, D. Burrows, J.S. Gallagher, J.R. Graham, M. Halverson, A. Kader, F.C. Michel, P. Scowen, Astrophys. J. **577**, L49 (2002)
K. Hirotani, Astrophys. J. **619**, 73 (2005)
K. Hirotani, I. Okamoto, Astrophys. J. **497**, 563 (1998)
T. Hovatta, E. Valtaoja, M. Tornikoski, A. Lähteenmäki, Astron. Astrophys. **498**, 723 (2009)
H. Ji, M. Burin, E. Schartman, J. Goodman, Nature **444**, 343 (2006)
T.W. Jones, S.L. O'Dell, Astrophys. J. **214**, 522 (1977)
S.G. Jorstad et al., Astron. J. **130**, 1418 (2005)
J. Kataoka, L. Stawarz, Astrophys. J. **622**, 797 (2005)
S.X. Kato, T. Kudoh, K. Shibata, Astrophys. J. **565**, 1035 (2002)
R. Keppens, Z. Meliani, B. van der Holst, F. Casse, Astron. Astrophys. **486**, 663 (2008)
S.S. Komissarov, N. Vlahakis, A. Königl, M.V. Barkov, Mon. Not. R. Astron. Soc. **394**, 1182 (2009)
C. Konar, M.J. Hardcastle, Mon. Not. R. Astron. Soc. **395**, 457 (2013)
A. Königl, R. Salmeron, M. Wardle, Mon. Not. R. Astron. Soc. **401**, 479 (2010)
E. Körding, M. Rupen, C. Knigge, R. Fender, V. Dhawan, M. Templeton, T. Muxlow, Science **320**, 1318 (2008). 2008
E. Körding, C. Knigge, T. Tzioumis, R. Fender, Mon. Not. R. Astron. Soc. **418**, L129 (2011)
R. Krasnopolsky, Z.-Y. Li, R.D. Blandford, Astrophys. J. **526**, 631 (1999)
T. Kudoh, R. Matsumoto, K. Shibata, Astrophys. J. **508**, 186 (1998)
T. Kuwabara, K. Shibata, T. Kudoh, R. Matsumoto, Astrophys. J. **621**, 921 (2005)
R.A. Laing, Mon. Not. R. Astron. Soc. **193**, 439 (1980)
R.A. Laing, A.H. Bridle, Mon. Not. R. Astron. Soc. **336**, 328 (2002)
R.A. Laing, A.H. Bridle, Mon. Not. R. Astron. Soc. **437**, 3405 (2014)
J.P. Leahy et al., Mon. Not. R. Astron. Soc. **291**, 20 (1997)
G. Lesur, P.-Y. Longaretti, Mon. Not. R. Astron. Soc. **378**, 1471 (2007)

Author's personal copy

G. Lesur, P.-Y. Longaretti, Astron. Astrophys. **504**, 309 (2009)
G. Lesur, J. Ferreira, G.I. Ogilvie, Astron. Astrophys. **550**, A61 (2013)
Z.-Y. Li, Astrophys. J. **415**, 118 (1993)
Z.-Y. Li, Astrophys. J. **444**, 848 (1995)
M.L. Lister, D.C. Homan, Astron. J. **130**, 1389 (2005)
M.L. Lister et al., Astron. J. **138**, 1874 (2009)
M.L. Lister et al., Astron. J. **146**, 120 (2013)
A.P. Lobanov, Astron. Astrophys. **330**, 79 (1998)
R.V.E. Lovelace, M.M. Romanova, G.V. Ustyugova, A.V. Koldoba, Mon. Not. R. Astron. Soc. **408**, 2083 (2010)
S.H. Lubow, J.C.B. Papaloizou, J.E. Pringle, Mon. Not. R. Astron. Soc. **267**, 235 (1994)
D. Lynden-Bell, Nature **223**, 690 (1969)
D. Lynden-Bell, J.E. Pringle, Mon. Not. R. Astron. Soc. **168**, 603 (1974)
M. Lyutikov, V.I. Pariev, D.C. Gabuzda, Mon. Not. R. Astron. Soc. **360**, 869 (2005)
A.P. Marscher, Astrophys. J. **264**, 296 (1983)
H.L. Marshall et al., Astrophys. J. Suppl. Ser. **193**, 15 (2011)
J.C. McKinney, Astrophys. J. **630**, L5 (2005)
J.C. McKinney, Mon. Not. R. Astron. Soc. **368**, 1561 (2006)
J.C. McKinney, C.F. Gammie, Astrophys. J. **611**, 977 (2004)
J.C. McKinney, A. Tchekhovskoy, R.D. Blandford, Mon. Not. R. Astron. Soc. **423**, 3083 (2012)
B.R. McNamara, F. Kazemzadeh, D.A. Rafferty et al., Astrophys. J. **698**, 594 (2009)
B.R. McNamara, M. Rohanizadegan, P.E.J. Nulsen, Astrophys. J. **727**, 39 (2011)
K. Meisenheimer, M.G. Yates, H.-J. Röser, Astron. Astrophys. **325**, 57 (1997)
Z. Meliani, F. Casse, C. Sauty, Astron. Astrophys. **460**, 1 (2006)
A. Mignone, P. Rossi, G. Bodo, A. Ferrari, S. Massaglia, Mon. Not. R. Astron. Soc. **402**, 7 (2010)
B. Mingo et al., Mon. Not. R. Astron. Soc. **440**, 269 (2014)
L.M. Mullin, M.J. Hardcastle, Mon. Not. R. Astron. Soc. **398**, 1989 (2009)
G.C. Murphy, J. Ferreira, C. Zanni, Astron. Astrophys. **512**, 82 (2010)
R. Narayan, I.V. Igumenshchev, M.A. Abramowicz, Proc. Astron. Soc. Jpn. **55**, L69 (2003)
R. Narayan, A. Sädowski, R.F. Penna, A.K. Kulkarni, Mon. Not. R. Astron. Soc. **426**, 3241 (2012)
R.S. Nemmen, A. Tchekhovskoy, arXiv:1406.7420 (2014)
E.E. Nokhrina, V.S. Beskin, Y.Y. Kovalev, A.A. Zheltoukhov, Mon. Not. R. Astron. Soc. **447**, 2726 (2015)
M.L. Norman, K.-H.A. Winkler, L.L. Smarr, M.D. Smith, Astron. Astrophys. **113**, 285 (1982)
S.P. O'Sullivan, D.C. Gabuzda, Mon. Not. R. Astron. Soc. **393**, 429 (2009a)
S.P. O'Sullivan, D.C. Gabuzda, Mon. Not. R. Astron. Soc. **400**, 26 (2009b)
R. Ouyed, R.E. Pudritz, Astrophys. J. **482**, 710 (1997)
R. Ouyed, D.A. Clarke, R.E. Pudritz, Astrophys. J. **582**, 292 (2003)
M.S. Paoletti, D.P. Lathrop, Phys. Rev. Lett. **106**, 024501 (2011)
G.G. Pavlov, M.A. Teter, O. Kargaltsev, D. Sanwal, Astrophys. J. **591**, 1157 (2003)
G. Pelletier, R.E. Pudritz, Astrophys. J. **394**, 117 (1992)
O. Porth, Mon. Not. R. Astron. Soc. **429**, 2482 (2013)
O. Porth, Ch. Fendt, Astrophys. J. **709**, 1100 (2010)
O. Porth, Ch. Fendt, Z. Meliani, B. Vaidya, Astrophys. J. **709**, 1100 (2011)
D. Proga, T.R. Kallman, Astrophys. J. **616**, 688 (2004)
D. Proga, J.M. Stone, T.R. Kallman, Astrophys. J. **543**, 686 (2000)
R.E. Pudritz, C.A. Norman, Astrophys. J. **274**, 677 (1983)
R.E. Pudritz, C. Rogers, R. Ouyed, Mon. Not. R. Astron. Soc. **365**, 1131 (2006)
R.E. Pudritz et al., in *Protostars and Planets V*, ed. by B. Reipurth, D. Jewitt, K. Keil (University of Arizona Press, Tucson, 2007)
R.E. Pudritz, M.J. Hardcastle, D.C. Gabuzda, Space Sci. Rev. **169**, 27 (2012)
A.B. Pushkarev, T. Hovatta, Y.Y. Kovalev et al., Astron. Astrophys. **545**, A113 (2012)
J.P. Ramsey, D.A. Clarke, Astrophys. J. **728**, 11 (2011)
S. Rawlings, R. Saunders, Nature **349**, 138 (1991)
M.J. Rees, M.C. Begeman, R.D. Blandford, E.S. Phinney, Nature **295**, 17 (1982)
R. Salmeron, A. Königl, M. Wardle, Mon. Not. R. Astron. Soc. **412**, 1163 (2011)
T. Savolainen, K. Wiik, E. Valtaoja, M. Tornikoski, in *Extragalactic Jets: Theory and Observation from Radio to Gamma Ray*, ed. by T.A. Rector, D.S. De Young (2008), p. 451
T. Savolainen, D.C. Homan, T. Hovatta, M. Kadler, Y.Y. Kovalev, M.L. Lister, E. Ros, J.A. Zensus, Astron. Astrophys. **512**, A24 (2010)
E. Schartman, H. Ji, M. Burin, J. Goodman, Astron. Astrophys. **543**, A94 (2012)
P.A.G. Scheuer, Mon. Not. R. Astron. Soc. **166**, 513 (1974)

Author's personal copy

N.I. Shakura, R.A. Sunyaev, Astron. Astrophys. **24**, 337 (1973)
H. Shang, Z.-Y. Li, N. Hirano, in *Protostars and Planets V*, ed. by B. Reipurth, D. Jewitt, K. Keil (University of Arizona Press, Tucson, 2007)
S. Sheikhnezami, Ch. Fendt, O. Porth, B. Vaidya, J. Ghanbari, Astrophys. J. **757**, 65 (2012)
K. Shibata, Y. Uchida, Proc. Astron. Soc. Jpn. **37**, 31 (1985)
J.B. Simon, J.F. Hawley, Astrophys. J. **707**, 833 (2009)
J.B. Simon, J.F. Hawley, K. Beckwith, Astrophys. J. **690**, 974 (2009)
N. Soker, J.P. Lasota, Astron. Astrophys. **422**, 1039 (2004)
K.V. Sokolovsky et al., Astron. Astrophys. **532**, A38 (2011)
D. Stepanovs, Ch. Fendt, Astrophys. J. **793**, 31 (2014)
D. Stepanovs, Ch. Fendt, S. Sheikhnezami, Astrophys. J. **796**, 29 (2014)
I.W. Stephens, L.W. Looney, W. Kwon, M. Fernández-López, A.M. Hughest, L.G. Mundy, R.M. Crutcher, Z.-Y. Li, R. Rao, Nature **514**, 597 (2014)
J.M. Stone, P.E. Hardee, Astrophys. J. **540**, 192 (2000)
J.M. Stone, M.L. Norman, Astrophys. J. **389**, 297 (1992)
J.M. Stone, M.L. Norman, Astrophys. J. **433**, 746 (1994)
T.K. Suzuki, S.-I. Inutsuka, Astrophys. J. **784**, 121 (2014)
F. Tavecchio, L. Maraschi, R.M. Sambruna, C.M. Urry, Astrophys. J. **544**, L23 (2000)
G.B. Taylor, R. Zavala, Astrophys. J. **722**, L183 (2010)
A. Tchekhovskoy, Launching of active galactic nuclei jets, in *The Formation and Disruption of Black Hole Jets*, ed. by I. Contopoulos, D. Gabuzda, N. Kylafis. Astrophysics and Space Science Library, vol. 414 (Springer, Berlin, 2015), pp. 45–82, Chapter 3. doi:10.1007/978-3-319-10356-3_3
A. Tchekhovskoy, D. Giannios, Mon. Not. R. Astron. Soc. **447**, 327 (2014)
A. Tchekhovskoy, J.C. McKinney, R. Narayan, Mon. Not. R. Astron. Soc. **388**, 551 (2008)
A. Tchekhovskoy, J.C. McKinney, R. Narayan, Astrophys. J. **699**, 1789 (2009)
A. Tchekhovskoy, R. Narayan, J.C. McKinney, New Astron. **15**, 749 (2010a)
A. Tchekhovskoy, R. Narayan, J.C. McKinney, Astrophys. J. **711**, 50 (2010b)
A. Tchekhovskoy, R. Narayan, J.C. McKinney, Mon. Not. R. Astron. Soc. **418**, L79 (2011)
A. Tchekhovskoy, J.C. McKinney, R. Narayan, J. Phys. Conf. Ser. **372**, 012040 (2012). arXiv:1202.2864
A. Tchekhovskoy, B.D. Metzger, D. Giannios, L.Z. Kelley, Mon. Not. R. Astron. Soc. **437**, 2744 (2014)
Y. Todo, Y. Uchida, T. Sato, R. Rosner, Astrophys. J. **403**, 164 (1993)
I.L. Tregillis, T.W. Jones, D. Ryu, Astrophys. J. **601**, 778 (2004)
P. Tzeferacos, A. Ferrari, A. Mignone, C. Zanni, G. Bodo, S. Massaglia, Mon. Not. R. Astron. Soc. **400**, 820 (2009)
P. Tzeferacos, A. Ferrari, A. Mignone, C. Zanni, G. Bodo, S. Massaglia, Mon. Not. R. Astron. Soc. **428**, 3151 (2013)
Y. Uchida, K. Shibata, Proc. Astron. Soc. Jpn. **36**, 105 (1984)
Y. Uchida, K. Shibata, Proc. Astron. Soc. Jpn. **37**, 515 (1985)
G.V. Ustyugova, A.V. Koldoba, M.M. Romanova, V.M. Chechetkin, R.V.E. Lovelace, Astrophys. J. **439**, 39 (1995)
G.V. Ustyugova, A.V. Koldoba, M.M. Romanova, V.M. Chechetkin, R.V.E. Lovelace, Astrophys. J. **516**, 221 (1999)
B. Vaidya, Ch. Fendt, H. Beuther, O. Porth, Astrophys. J. **742**, 56 (2011)
A.A. van-Ballegooijen, in *Accretion Disks and Magnetic Fields in Astrophysics*, ed. by G. Belvedere (1989), p. 99
B. von Rekowski, A. Brandenburg, Astron. Astrophys. **420**, 17 (2004)
B. von Rekowski, A. Brandenburg, W. Dobler, Astron. Astrophys. **398**, 825 (2003)
M. Wardle, A. Königl, Astrophys. J. **410**, 218 (1993)
J.F.C. Wardle, D.C. Homan, R. Ojha, D.H. Roberts, Nature **395**, 457 (1998)
W.F. Winters, S.A. Balbus, J.F. Hawley, Mon. Not. R. Astron. Soc. **340**, 519 (2003)
S. Wykes et al., Astron. Astrophys. **558**, A19 (2013)
M. Zamaninasab, E. Clausen-Brown, T. Savolainen, A. Tchekhovskoy, Nature **510**, 126 (2014)
C. Zanni, A. Ferrari, R. Rosner, G. Bodo, S. Massaglia, Astron. Astrophys. **469**, 811 (2007)
A.A. Zdziarski, M. Sikora, P. Pjanka, A. Tchekhovskoy, Mon. Not. R. Astron. Soc. **451**, 927 (2015)
H. Zinnecker, M.J. McCaughrean, J.T. Rayner, Nature **394**, 862 (1998)